

1 **Disturbance Triggers Non-Linear Microbe-Environment Feedbacks**

2 Aditi Sengupta^{1†}, Sarah J. Fansler^{2†}, Rosalie K. Chu³, Robert E. Danczak², Vanessa A. Garayburu-Caruso², Lupita
3 Renteria², Hyun-Seob Song⁴, Jason Toyoda³, Jacqueline Wells⁵, and James C. Stegen^{2*}

4 [†]Denotes equal contribution

5 ¹California Lutheran University, Thousand Oaks, CA

6 ²Pacific Northwest National Laboratory, Ecosystem Science Team, Richland, WA

7 ³Environmental Molecular Sciences Laboratory, Richland, WA

8 ⁴University of Nebraska-Lincoln, Lincoln, NE

9 ⁵Oregon State University, Corvallis, OR

10 *Correspondence to:* James Stegen (James.Stegen@pnnl.gov)

11 **Abstract**

12 Conceptual frameworks linking microbial community membership, properties, and processes with the
13 environment and emergent function have been proposed but remain untested. Here we refine and test a
14 recent conceptual framework using hyporheic zone sediments exposed to wetting/drying transitions. Our
15 refined framework includes relationships between cumulative properties of a microbial community (*e.g.*
16 microbial membership, community assembly properties, and biogeochemical rates), environmental
17 features (*e.g.* organic matter thermodynamics), and emergent ecosystem function. Our primary aim was
18 to evaluate the hypothesized relationships that comprise the conceptual framework and contrast outcomes
19 from the whole and putatively active bacterial and archaeal communities. Throughout the system we found
20 threshold-like responses to the duration of desiccation. Membership of the putatively active bacterial
21 community--but not the whole bacterial and archaeal community--responded due to enhanced
22 deterministic selection (an emergent community property). Concurrently, the thermodynamic properties
23 of organic matter (OM) became less favorable for oxidation (an environmental component) and respiration
24 decreased (a microbial process). While these responses were step functions of desiccation, we found that
25 in deterministically assembled active communities, respiration was lower and thermodynamic properties
26 of OM were less favorable. Placing the results in context of our conceptual framework points to previously

27 unrecognized internal feedbacks that are initiated by disturbance, mediated by thermodynamics, and that
28 cause the impacts of disturbance to be dependent on the history of disturbance.

29

30

1 Introduction

31

1.1 Conceptual Foundations

32 Given the influence of microbes over ecosystem function, deeper knowledge of microbe-environment
33 relationships is needed to improve ecosystem models (Bier et al., 2015). In turn, there is strong interest
34 in quantifying and predicting microbe-environment relationships such as defining microbial life history
35 strategies as traits in ecosystem models (Malik et al., 2020), assessing microbial biomass stoichiometry
36 distributions in response to changing resource environments (Manzella et al., 2019), and evaluating the
37 extent of microbial adaptation to changing environments and their role in biogeochemical processes
38 (Wallenstein and Hall, 2012). To enhance and synthesize understanding of microbe-environment
39 interactions, it is useful to develop conceptual frameworks based on linkages among microbial
40 characteristics and ecosystem processes. Previous work has used such frameworks to improve
41 mechanistic representation and predictive capacity of microbe-environment interactions in ecosystem
42 models (Wieder et al., 2015).

43

44 A recently developed framework by Hall et al. (2018) poses a series of concepts that collectively define
45 the intersection between microbial and ecosystem ecology. Their framework draws attention to causal
46 relationships between microbial characteristics (microbial membership influences community properties
47 and microbial processes), which in turn regulate ecosystem fluxes. These components can be further
48 modified by environmental variation leading to cumulative ecosystems processes with the potential to
49 incorporate relevant mechanistic links into predictive ecosystem models. Hall et al. (2018) particularly

50 draws attention to the need to understand how microorganisms influence their environment by
51 separating microbial community properties based on community aggregated traits (those which can be
52 predicted using constituent taxa) and emergent properties (properties unable to be explained by
53 constituent taxa). A powerful element of the framework is that it applies to diverse systems spanning
54 natural (Gilbert et al., 2018), host-associated (Lloyd-Price et al., 2019), and built (Fu et al., 2020)
55 environments as well as across spatiotemporal scales (König et al., 2018). While potentially very useful,
56 the Hall et al. (2018) framework has seen little direct use in terms of explicitly defining and evaluating
57 the linkages within specific study systems (but see Manzella et al., 2019). To make full use of and
58 continually improve the framework, it is necessary to consider different realizations and interpretations
59 of the proposed linkages. In the following paragraphs we detail a modified interpretation of the
60 framework (**Fig. 1**) to enable its application to microbial communities and biogeochemistry associated
61 with hyporheic zone sediments experiencing hydrological disturbance. In turn, we use data from a
62 controlled laboratory experiment to evaluate key linkages within the modified framework.

63

64 Our modified framework aims to refine the link between microbial communities and ecosystem
65 functions. As detailed below, a couple critical elements of our modification include:
66 Defining and evaluating the relative influence of community assembly processes as an emergent
67 community property, and ii) proposing bi-directional links between environment and microbial
68 processes to indicate that environmental conditions drive microbial processes, which in turn influence
69 the environment, and these cumulative environment-microbial processes ultimately drive ecosystem
70 function.

71

72 1.2 Conceptual Framework Development

73 As in Hall et al. (2018) we consider microbial membership to be directly influenced by environmental
74 conditions (arrow 4, Fig.1) and to underlie community-level properties (arrow 1, Fig. 1). Determining
75 microbial membership is relatively straightforward, and uses culture-independent (Behrens et al., 2012;
76 Norland et al., 1995; Thompson et al., 2017; Wagner, 2009) and culture-dependent (Bartelme et al.,
77 2020) techniques. Sequence-based assays using phylogenetic markers are routine, with DNA-based
78 (total community members) and RNA-based (putatively active community members) (Barnard et al.,
79 2015; Blazewicz et al., 2013; Cardoso et al., 2017; Kearns et al., 2016; Shu et al., 2019; Wisnoski et al.,
80 2020) approaches providing the foundation to study community properties.

81

82 While community membership is relatively straightforward, the identification of community properties
83 that are relevant to a given system and function is open to broader interpretation. Here we propose using
84 the relative influences of deterministic and stochastic community assembly processes (Stegen et al.,
85 2012) as emergent properties of microbial communities that have implications for biogeochemical
86 function (Graham and Stegen, 2017) including in ecosystems experiencing environmental disturbance.
87 Deterministic mechanisms are associated with systematic differences in reproductive success imposed
88 by the biotic and/or abiotic environment, while stochastic mechanisms are associated with passive
89 spatial movements of organisms and birth/death events that are not due to systematic differences across
90 taxa in reproductive success (Dini-Andreote et al., 2015; Stegen et al., 2015). The relative contributions
91 of determinism and stochasticity can be inferred by coupling microbial community membership and
92 phylogeny to ecological null models (Stegen et al., 2012, 2013, 2015; Zhou and Ning, 2017).

93

94 We propose that the relative contributions of determinism and stochasticity are emergent properties that
95 are greater than the sum of the individual components (i.e., taxa), and that are complementary to the

96 community properties proposed by Hall et al. (Hall et al., 2018), such as biomass and gene expression.
97 Furthermore, we propose that there are feedbacks between assembly processes and microbial
98 membership whereby assembly processes influence which taxa are found in which abundances, but
99 biotic interactions also influence assembly processes. In turn, we modified the framework whereby
100 arrow 1 is bidirectional (Fig. 1).

101
102 It is important to recognize that the ecological processes of community assembly are distinct from
103 'microbial processes' associated with biogeochemical reactions. As an emergent property, the relative
104 influence of determinism and stochasticity is the result of complex biotic and abiotic interactions (Grilli
105 et al., 2017) and also shapes cumulative microbial processes that impact ecosystem biogeochemical
106 functions (Graham and Stegen, 2017) (arrow 2, Fig.1). For example, a stronger influence of determinism
107 over community assembly is hypothesized to cause higher respiration rates (a microbial processes) due
108 to a larger contribution of well-adapted taxa (Graham and Stegen, 2017), though the respiration response
109 may vary depending on the existing community composition and the deterministic forces exerted.

110
111 Analyses of microbial community assembly have been widely employed across environments including
112 soil (Bottos et al., 2018; Dini-Andreote et al., 2015; Feng et al., 2018; Jurburg et al., 2017; Sengupta et
113 al., 2019b), sediment (Graham et al., 2017a; Stegen et al., 2013, 2016, 2018b), marine (Starnawski et al.,
114 2017; Wu et al., 2018), riverine (Chen et al., 2019), gut (Martínez et al., 2015), and engineered (Ofișeru
115 et al., 2010; Zhou et al., 2013) systems. Previous work has focused primarily on using DNA-derived
116 membership and phylogenetic data to study whole-community assembly. In contrast, recent studies have
117 also used an RNA-based approach to study the relative influence of stochasticity over the assembly of
118 the putatively active portion of microbial communities (Jia et al., 2020; Jurburg et al., 2017). This RNA-

119 based approach is complementary to the DNA-based approach and may provide additional insights into
120 shorter-term dynamic linkages between emergent community properties and microbial processes. Such
121 linkages have not, however, been previously evaluated.

122

123 The Hall et al. (2018) framework proposes that microbial processes (e.g., respiration rate) are
124 influenced by both microbial community properties and environmental factors. Here we propose a
125 revision of this structure that includes bidirectional links between the environment and microbial
126 processes (arrow 3, Fig. 1). Such bi-directional links between microbes and their environment are
127 common (Daly et al., 2016; Leventhal et al., 2019; Ratzke et al., 2018; Stegen et al., 2018a), and in
128 hyporheic zone sediments may be particularly tied to thermodynamic properties of organic matter
129 (Graham et al., 2018) and influenced by hydrological disturbances that are common in such
130 environments. For example, preferential use of OM by microbial communities has potential to alter the
131 thermodynamic properties of organic matter pools (Graham et al., 2017a). This microbe-driven shift in
132 the environment could then feedback to impact microbial metabolism due to the strong influence of OM
133 thermodynamics on biogeochemical rates (Boye et al., 2017; Garayburu-Caruso et al., 2020; Song et al.,
134 2020; Stegen et al., 2018b). Bi-directional feedback between environmental factors and microbial
135 processes is, therefore, likely important to the link between microbial communities and ecosystem
136 function. Fundamental knowledge of these feedbacks and how they are modulated by hydrologic
137 disturbances in hyporheic zone sediments is largely unknown, however.

138

139 Within ecosystems, mechanistic associations between environmental factors, microbial properties, and
140 microbial processes underlie spatial and temporal distributions of biogeochemical rates (Fig. 1 arrow 5).
141 The resulting distributions (e.g., of respiration rates) define cumulative system function and can be used

142 to understand key phenomena such as biogeochemical hot spots and hot moments (McClain et al.,
143 2003). Developing concepts and models to predict the influences of biogeochemical hot spots/moments
144 is a major outstanding challenge. To facilitate progress, Bernhardt et al. (2017) proposed grouping hot
145 spots/moments into the concept of ecosystem control points that exert a disproportionate influence on
146 ecosystem function.

147

148 While not called out explicitly in Bernhardt et al. (2017), the control point concept is based on the
149 distribution of biogeochemical rates through space and/or time. Focusing on the shape of rate
150 distributions allows the notion of control points to be extended to the concept of control point influence
151 (CPI; Fig. 1 arrow 5). The CPI is a quantitative measurement of the contribution of elevated
152 biogeochemical rates in space and/or time to the net aggregated rate within a defined system (Arora et
153 al., 2020). While proposed conceptually and studied via simulation in Arora et al. (2020), empirical
154 measurements of CPI are lacking. More generally, incorporating CPI into a modified version of the Hall
155 et al. (2018) framework (Fig. 1), provides an integrated conceptualization for how environmental
156 factors, microbial properties, and microbial processes contribute to emergent system function.

157

158 Some elements of our modified framework (Fig. 1) are generalizable across systems (e.g., CPI), while
159 others (e.g., OM thermodynamics) may have different levels of relevance across different ecosystem
160 types. Here we aim to generate fundamental knowledge of the linkages between microbial community
161 and ecosystem function, as well as reveal how hydrologic disturbance may modify these linkages. While
162 relationships between microbial community assembly and function have been evaluated, integrating the
163 concepts of microbial structure, function, assembly, and environment interactions into one coherent

164 framework has the potential to advance our understanding of the feedbacks between microbial
165 communities and the environment.

166

167 1.3 Study Objectives

168 Our primary objective was to study the modified conceptual framework in context of variably inundated
169 hyporheic zone sediments exposed to different drying/wetting dynamics. Hyporheic zones are
170 biogeochemically active subsurface domains in river corridors through which surface water flows and
171 can mix with groundwater (Bernhardt et al., 2017; Boano et al., 2014; McClain et al., 2003). These
172 zones can have disproportionate biogeochemical impacts on river corridors (Boano et al., 2014; Burrows
173 et al., 2017; Demars, 2019; Fischer et al., 2005; Kaufman et al., 2017). Within variably inundated
174 streams (Larned et al., 2010; Romaní et al., 2006), hyporheic zones experience extreme changes in
175 environmental conditions, but the consequences of this variability for microbe-ecosystem linkages is
176 poorly known.

177

178 To mimic natural disturbances, we subjected sediments to wetting-drying transitions and focused on a
179 series of analyses tied to our modified framework. We specifically evaluated relationships between: (i)
180 the relative influence of stochastic assembly as a community property and respiration rates as a
181 microbial process (Fig. 1 arrow 2), and (ii) environmental features and both microbial properties (Fig. 1
182 arrow 4) and processes (Fig. 1 arrow 3) that underlie aggregate system function (Fig. 1 arrow 5). We
183 evaluated relationships between cumulative properties of the microbial community (membership,
184 assembly, biogeochemical rates), environmental features, and emergent ecosystem function by
185 hypothesizing that: (i) Stronger influences of determinism result in well-adapted microbes that will
186 generate higher respiration rates, (ii) Longer duration in an inundated state will result in greater
187 influences of stochastic assembly--due to weaker ecological selection--and lower respiration rates

188 following re-inundation due to relatively consistent abiotic conditions (Birch, 1964), (iii) Microbial
189 processes are facilitated by OM that is thermodynamically more favorable for oxidation, leading to an
190 association between respiration rates and OM thermodynamics, and (iv) More wet/dry transitions will
191 increase among-replicate heterogeneity (e.g., in microbial membership) thereby increasing CPI by
192 increasing within-treatment variability in respiration rates.

193

194 2 Methods

195 2.1 Study site and sediment collection

196 Hyporheic sediments were collected from the Columbia River shoreline (approximately 46.372411°N,
197 119.271695°W) in eastern Washington State (Fig S1) (Arntzen, 2006; Goldman et al., 2017; Graham et
198 al., 2016; Slater et al., 2010; Stegen et al., 2018b; Zachara et al., 2013) within the Hanford Site on
199 January 14, 2019 at 9 am Pacific Standard Time. Samples were aseptically collected to a depth of 10 cm
200 at five sub-sampling locations within a meter to form a composite sample that was sieved on site
201 through a 2 mm sieve into a clean glass beaker. Sieved sediment was stored on blue ice for 30 min while
202 being transported back to the laboratory. Once back at the laboratory sediment was stored at 4 °C until
203 processing into incubation vials (see below).

204

205 The sediments were subjected to increasing temporal environmental variance (as a function of periodic
206 wetting and drying transitions) and evaluated for associations between microbial membership, microbial
207 properties, microbial community assembly, OM chemistry, absolute respiration rate (represented in this
208 study as O₂ consumption rates), and cumulative respiration rates represented as CPI. Aerobic respiration
209 was chosen as the biogeochemical process since it influences global-scale energy and material fluxes

210 (Fatichi et al., 2019), and because the hyporheic zone within the field system is predominantly aerobic
211 (Graham et al., 2016, 2017b). Detailed experimental design and methods are provided in the following
212 paragraphs.

213

214 2.2 Experimental design

215 Sediments used in the batch reactors were sourced from one homogenized sediment pool. In turn, 10 g
216 of sediment from the homogenized pool was added to each reactor vial. The sample set was then split
217 into two groups, one inundated and the other allowed to desiccate. Desiccation was achieved within 15-
218 17 days. Sediments were periodically weighed to allow the inundated samples to be maintained at a
219 constant water content and to monitor the remaining samples for desiccation. Inundated sediments were
220 placed on ceramic porous plates saturated with DI water for weight adjustments. These conditions were
221 maintained for 23 days prior to the start of dynamic moisture manipulation, from January 29th to
222 February 21st, 2019. This initial ‘preconditioning’ period was used to avoid measuring the immediate
223 impacts of sampling disturbance and to allow time for desiccation. All replicate reactors were
224 maintained in the dark, shaking at 100 rpm, at 21 °C and were covered with a gas permeable Breathe-
225 Easy (Milli-Pore Sigma, Burlington, MA) membrane that allowed for gas exchange and drying. After
226 the preconditioning period in which sediments were consistently inundated or allowed to continuously
227 desiccate, the transition regimes (**Fig. 2**) were applied to the reactors starting on February 22nd, 2019.
228 We refer to the time from Feb 22nd, 2019 onwards as the ‘transitions period’ for all treatments, even
229 though some did not experience transitions between being inundated and dry. Each treatment had 6-7
230 replicates (detailed below). These regimes were designed around the number of wet/dry transitions
231 experienced by sediments within a given treatment. Treatment regimes also caused variation in the

232 cumulative number of days sediments were in a drying state. We imposed six different experimental
233 treatment regimes (**Fig. 2**) as follows:

- 234 • 0 Transitions and 0 days of desiccation: Sediments were maintained at field moisture conditions
235 for the preconditioning and transitions periods. This treatment had 6 replicates.
- 236 • 1 Transition and 34 days of desiccation: Sediments were dry during the preconditioning and
237 transitions periods, and transitioned once to the field moisture level prior to respiration
238 estimation. This treatment had 6 replicates.
- 239 • 2 Transitions and 4 days of desiccation: Sediments were held at field moisture levels for the
240 preconditioning period and then for the first 7 days of the transitions period, then transitioned to
241 a dried state for 4 days, and transitioned to field moisture conditions prior to respiration
242 estimation. This treatment had 7 replicates.
- 243 • 3 Transitions and 31 days of desiccation: Sediments were dry during the preconditioning period
244 and the first 4 days of the transitions period, then transitioned to field moisture levels for three
245 days, then transitioned to 4 days in a dried state, and transitioned again to field moisture levels
246 prior to respiration estimation. This treatment had 7 replicates.
- 247 • 4 Transitions and 8 days of desiccation: Sediments were held at field moisture levels for the
248 preconditioning period and transitioned to a dried state for the first 4 days of the transitions
249 period, then transitioned to field moisture levels for 3 days, then transitioned to 4 days in a dried
250 state, and transitioned to field moisture levels prior to respiration estimation. This treatment had
251 7 replicates.
- 252 • 5 Transitions and 27 days of desiccation: Sediments were dry during the preconditioning period
253 and then transitioned to field moisture levels for the first 3 days of the transitions period,
254 transitioned to a dried state for 2 days, transitioned to field moisture levels for 2 days,

255 transitioned to a dried state for 2 days, and transitioned to field moisture levels for 3 days prior to
256 respiration estimation. This treatment had 7 replicates.

257

258 To avoid modifying electrical conductivity across experimental treatments, sterile deionized water was
259 added to reactors to achieve/maintain field moisture levels according to the defined wet/dry regimes
260 detailed above. For reactors with sediments that were below field moisture levels, deionized water was
261 added to achieve field moisture levels prior to respiration rate estimation. Changes in the total mass of
262 reactors and volumes of water added during the course of the experiment are provided in Table S1.

263

264 2.3 Respiration rate measurements

265 Laboratory incubations were performed in batch reactors to quantify dissolved oxygen consumption
266 rates. Borosilicate glass vials (20 ml) (I-Chem™ Clear VOA Glass Vials, Thermo-Fisher, Waltham,
267 MA) served as incubator reactors. Factory calibrated oxygen sensor spots (Part# 200001875, diameter =
268 0.5 cm, detection limit 15 ppb, 0 – 100 % oxygen; PreSens GmbH, Regensburg, Germany) were adhered
269 to the inner vials of the reactor prior to sediment addition. Detailed description of sensor adhesion and
270 non-destructive measurements of DO consumption using these sensors is provided in Garayburo-Caruso
271 et al. (Garayburo-Caruso et al., 2020). Vials were grouped into six treatment regimes (explained in the
272 previous section) representing inundation-drought transitions.

273

274 Sample processing and incubations were performed in a laboratory at 21 ± 1 °C. The reactors were
275 monitored for 2 hours, with measurement of dissolved oxygen (DO) concentration ($\mu\text{mol L}^{-1}$) every 30
276 min. DO concentration in each bioreactor was measured with an oxygen optical meter (Fibox 3;

277 PreSens GmbH) connected to a 2 mm polymer optical fiber lined up to sense the sensor dot every thirty
278 minutes. A few samples were discarded due to sensor dots detaching from the glass surface. Respiration
279 rates ($\mu\text{mol L}^{-1} \text{ h}^{-1}$) were estimated as the slope of the linear regression between DO concentration and
280 incubation time for each sample. Some non-linearity was observed in the relationship between DO
281 concentration and time such that only the first 4 data points--time zero to 2 hours--were used to fit a
282 linear function. The slope of the linear function was taken as an estimate of respiration rate.
283

284 2.4 Microbial Analysis

285 Post-incubation, the sediment slurry was transferred to centrifuge tubes (Item#28-108 Genesee
286 Scientific) and centrifuged for 5 min at 3200 rcf and 20°C. The supernatant was removed and reserved
287 for biogeochemistry analyses and sediment aliquots for DNA and RNA extraction were flash-frozen in
288 liquid N₂ and stored at -80 °C. The extraction, purification, and sequencing of sediment microbial
289 gDNA were performed according to published protocol (Bottos et al., 2018). The extraction of RNA was
290 performed using the Qiagen PowerSoil RNA extraction kit (Qiagen, Germantown, MD). RNA was
291 treated with DNase and quantified with a Qubit RNA kit (Thermo Fisher, Waltham, MA). An aliquot of
292 the RNA extraction was used to generate cDNA using SuperScript™ IV First-Strand Synthesis System
293 (Thermo Fisher Scientific, Waltham, MA). The 16S rRNA gene sequencing--for both gDNA and
294 cDNA--followed the established protocol by The Earth Microbiome Project (Caporaso, 2018). Sequence
295 pre-processing, operational taxonomic unit (OTU) assignment, and phylogenetic tree building were
296 performed using an in-house pipeline, HUNDO (Brown et al., 2018). Sequences were deposited at
297 NCBI's Sequence Read Archive PRJNA641165. The final sample count of gDNA and cDNA,
298 respectively, for each treatment regime, after dropping samples following quality filtering and

299 rarefaction, was 5 and 5 (0 transition), 4 and 3 (1 transition), 5 and 4 (2 transitions), 7 and 6 (3
300 transitions), 7 and 6 (4 transitions), and 7 and 5 (5 transitions). Rarefaction levels are provided below in
301 the Statistics section.

302

303 2.5 Biogeochemistry

304 Reserved supernatant was filtered through a 0.22 μm polyethersulfone membrane filter (Millipore
305 Sterivex) and an aliquot was immediately removed for non-purgeable organic carbon (NPOC) and the
306 remainder was stored at -20C until further OM high resolution analysis was conducted (see below).
307 NPOC was determined by acidifying an aliquot of sample with 15% by volume of 2N ultra-pure HCL
308 (Optima grade, Fisher#A466-500). The acidified sample was sparged with carrier gas (zero air, Oxarc#
309 X32070) for 5 minutes to remove the inorganic carbon component. The sparged sample was then
310 injected into the TOC-L furnace of the Shimadzu combustion carbon analyzer TOC-L CSH/CSN E100V
311 with ASI-L auto sampler at 680°C using 150 μL injection volumes. The best 4 out of 5 injections
312 replicates were averaged to get the final result. The NPOC standard was made from potassium
313 hydrogen phthalate solid (Nacalia Tesque, lot M7M4380). The calibration range was 0 to 70 ppm
314 NPOC as carbon.

315 Fourier Transform Ion Cyclotron Resonance Mass Spectrometry (FTICR-MS) of post-incubation
316 sediment slurry was conducted as per Danczak et al. (2020). Sample processing, injection, and data
317 acquisition, processing and analysis was performed as per scripts provided in Danczak et al. (2020), with
318 ‘Start tolerance’ in Formularity changed to 8. Ten samples were dropped due to poor calibration,

319 resulting in 5 replicates for 0 transition, 4 replicates for 1 transition, 5 replicates for 2 transitions, 6
320 replicates for 3 transitions, and 5 replicates each for 4 and 5 transition regimes.

321

322 From the FTICR-MS data, as in previous work (Garayburu-Caruso et al., 2020; Graham et al., 2018;
323 Sengupta et al., 2019b; Stegen et al., 2018b), we followed LaRowe and Van Cappellen (LaRowe and
324 Van Cappellen, 2011) to calculate the Gibbs free energy for the half reaction of organic carbon
325 oxidation under standard conditions (ΔG^0_{Cox}). This calculation is based on elemental stoichiometries
326 associated with molecular formulae assigned to individual molecules observed in the FTICR-MS data.

327 The formulae assignments are part of the processing scripts described in (Danczak et al., 2020). As in
328 previous work (Garayburu-Caruso et al., 2020; Graham et al., 2018; Sengupta et al., 2019b; Stegen et
329 al., 2018b), we interpret larger values of ΔG^0_{Cox} to indicate OM that is thermodynamically less favorable
330 for oxidation by microbes. That is, larger values of ΔG^0_{Cox} indicate OM that provides less net energy to a
331 microbial cell per oxidation event, assuming all else is equal. Given the large numbers of assigned
332 formulae within each sample, this resulted in thousands of ΔG^0_{Cox} estimates within each sample, from
333 which we estimated mean ΔG^0_{Cox} for each sample.

334

335 2.6 Estimating influences of community assembly processes

336 The relative influences of community assembly processes impacting microbial community membership
337 are emergent properties that cannot be calculated/inferred directly from knowledge of membership. To
338 evaluate assembly processes as a link between membership and microbial processes (refer Fig. 1) it is
339 necessary to quantitatively estimate the relative influences of these processes. To do so we use a well-
340 established null modeling framework based on phylogenetic relationships among microbial taxa (Dini-

341 Andreote et al., 2015; Stegen et al., 2012, 2015; Zhou and Ning, 2017). We refer the reader to these
342 previous studies for details. In brief, randomizations were used to generate estimates of phylogenetic
343 associations among microbial taxa for scenarios in which microbial communities were stochastically
344 assembled. These stochastic (i.e., null) expectations were compared quantitatively to observed
345 phylogenetic associations to estimate the β -Nearest Taxon Index (β NTI) (Stegen et al., 2012). We used
346 cDNA sequences rarefied to 27227 and gDNA sequences rarefied to 15106 sequences per sample to
347 determine putatively active community and whole community β NTI values, respectively. Samples
348 falling below these sequence counts were removed as indicated above in subsection 2.4 *Microbial*
349 *Analysis*. A β NTI value of 0 indicates no deviation between the stochastic expectation and the observed
350 phylogenetic associations, thereby indicating the dominance of stochastic assembly processes. As β NTI
351 deviates further from 0, there is an increasing influence of deterministic assembly processes that drive
352 community membership away from the stochastic expectation. β NTI values below -2 or above +2
353 indicate statistical significance, with negative and positive values indicating less than or more than
354 expected shifts in membership. β NTI is a pairwise metric measured between any two
355 communities/samples, such that shifts in membership are related to changes between the pair of
356 communities being evaluated. We used β NTI to study all pairwise community comparisons within each
357 experimental treatment. Each community from a given reactor is therefore associated with multiple
358 β NTI values due to being compared to communities associated with other replicate reactors. In turn, the
359 average β NTI was calculated for each reactor. As in Stegen et al. (Stegen et al., 2015), this provides a
360 community-specific value for β NTI and thus an estimate of the relative influences of stochastic and
361 deterministic processes causing deviations between a given community and all other communities within
362 the same experimental conditions (Sengupta et al., 2019b). That is, the larger the absolute value of β NTI
363 for a given community, the stronger the influence of deterministic assembly processes acting on that

364 community (Stegen et al., 2015). In turn, these community-specific estimates were related to reactor-
365 specific measurements. For example, respiration rates were regressed against β NTI to evaluate the link
366 between emergent properties (i.e., ecological assembly) and microbial processes (i.e., respiration rates).

367

368 2.7 Evaluating relationships between microbial characteristics and 369 environment

370 Respiration rate distributions, absolute β NTI values, and ΔG^0_{Cox} were summarized as box plots.
371 Pairwise Mann-Whitney test was performed to evaluate statistical differences between reactor-specific
372 measurements (e.g., respiration rates and thermodynamic properties) and treatment groups (cumulative
373 dry and inundated days). Continuous bivariate relationships were evaluated with ordinary least squares
374 regression. Prior to regression analyses, respiration rates were log-transformed due to non-linearities
375 resulting from respiration being constrained to be at or above zero. Prior to log-transformation, half the
376 smallest non-zero rate was added to each rate to enable inclusion of rate estimates with a value of zero.

377

378 2.8 Control point influence calculation

379 To characterize respiration rate distributions we used the control point influence (CPI) metric. CPI was
380 recently developed (Arora et al., 2020) and is defined as the fraction of cumulative function (R_{tot} ; e.g.,
381 total respiration rate) within a defined system that is contributed by individual rates that are above the
382 system's median rate (R_{med}). To define cumulative function one must first define the system being
383 evaluated. In our study, all replicate batch reactors within a given experimental treatment were
384 conceptualized as a representative set of samples from a larger system experiencing the experimental

385 conditions. R_{tot} for each treatment was therefore estimated as the sum of respiration rates across a
386 treatment's replicate reactors. CPI was estimated as the sum of respiration rates that fell above the
387 median rate for a given treatment (R_{above}) divided by R_{tot} for that treatment. That is, $R_{above} = \sum_i^N R_i$,
388 where R_i are respiration rates from individual reactors that fell above R_{med} , and $CPI = R_{above}/R_{tot}$.
389

390 An important feature of CPI is that it makes no assumptions of distribution normality, and can be
391 estimated for rate distributions of any form (e.g., unimodal, multimodal, Gaussian, skewed, etc.). In
392 most cases, CPI is constrained to have a minimum value of 0.5 (for a perfectly normal distribution with
393 no outliers) and asymptotically approach 1 as a maximum value (e.g., for heavily skewed distributions
394 with a small number of very high rates). CPI therefore quantitatively estimates the biogeochemical
395 contribution of places in space or points in time that have elevated biogeochemical rates.
396

397 Understanding how CPI varies through space, time, and with environmental conditions (e.g., disturbance
398 frequency) provides an opportunity to deepen our understanding of factors controlling hotspot/moment
399 behavior. Lower values of CPI (i.e., closer to 0.5) can arise through any mechanism that constrains
400 biogeochemical rates to be consistent through space or time. For example, if respiration rates were
401 measured in multiple locations across a well-mixed water body, we may expect a Gaussian rate
402 distribution with little variation. The cumulative respiration of the water body should not be influenced
403 significantly by hotspots, which would be reflected in low CPI. Conversely, higher values of CPI (i.e.,
404 closer to 1) can arise through any mechanism that increases the probability of positive outliers within a
405 given rate distribution. Spatial variation in the temporal dynamics of disturbances (e.g., more frequent
406 disturbances in some locations) is an example that is closely aligned with our experimental treatments.
407 In this case the probability of rate outliers (i.e., hotspots) may vary as a function of disturbance

408 frequency. For example, in spatial domains that experience more wetting/drying dynamics we might
409 expect a higher probability of rate outliers. This is because each time sediments go dry the exact spatial
410 distribution of water films that remain will vary across locations within the broader wetted/dried spatial
411 domain. In turn, we would expect higher values of CPI in spatial domains that are more frequently
412 wetted and dried. Regardless of whether this specific hypothesis is rejected or not, we contend that using
413 CPI enables development of *a priori* quantitative hypotheses spanning space, time, environmental
414 conditions (e.g., disturbance frequency), and scales. This provides new opportunities to more
415 systematically elucidate factors governing the influence of hotspots/moments.

416 3 Results

417 To link microbial membership to emergent microbial community properties (Fig. 1 arrow 1) we used
418 null modeling to estimate the contributions of stochastic and deterministic community assembly. Results
419 from the null models indicate a relatively balanced mixture of stochasticity and determinism for both the
420 whole community (gDNA-based) and putatively active community (rRNA-based) (Fig. S2). More
421 specifically, stochasticity and determinism each governed 50% of turnover in microbial membership for
422 the whole community and 33% and 67%, respectively, for the putatively active community. The relative
423 contributions of the two deterministic components (homogeneous and variable selection) were strongly
424 imbalanced. Homogeneous selection was responsible for 94% and 91% of the deterministic component
425 for the whole and putatively active communities, respectively. The contributions of homogeneous and
426 variable selection to the deterministic component must sum to 1, such that the variable selection was
427 responsible for 6% and 9% of the deterministic component for the whole and putatively active
428 communities, respectively.

429

430 As shown in Figure 1 (arrow 2), we hypothesized a link between microbial community properties and
431 microbial processes realized as a relationship between the strength of determinism and respiration rates.
432 Such a relationship was not observed for the whole community (Fig. 3a), but we did observe a non-
433 linear decreasing relationship between respiration rates and the absolute value of β NTI for the putatively
434 active community (Fig. 3b). The direction of this relationship (negative) was opposite of that expected,
435 and the relationship was clearly structured by among-treatment shifts in both respiration rate and β NTI
436 (Fig. 3b).

437

438 In our conceptual framework there are multiple ways in which connections among the environment,
439 microbial properties, and microbial processes may be realized, in part due to the environment having
440 multiple components relevant to our study (Fig. 1 arrows 3,4). More specifically, the environment was
441 characterized here in terms of both disturbance (number of dry days; imposed by the experimental
442 manipulation) and OM thermodynamics (ΔG^0_{Cox} ; this is an emergent aspect of the environment).

443

444 Disturbance influenced both microbial properties and processes. These influences appeared to be non-
445 linear with experimental treatments associated with the two largest number of dry days (31 and 34)
446 causing decreases in respiration rates (Fig. 4a) and stronger influences of deterministic homogeneous
447 selection for the putatively active community (Fig. 4b). Disturbance had no clear influence on
448 community assembly for the whole community (Figs. S3, S4a). Given the apparent binary nature of
449 these results, we evaluated statistical significance by combining respiration rate data from treatments
450 with 0-27 cumulative dry days and separately combining data from treatments with 31 or 34 cumulative
451 dry days (Fig. S5). Respiration rates were significantly depressed in the treatments associated with 31 or
452 34 cumulative dry days ($W = 5$, $p < 0.001$). The β NTI data are non-independent due to being based on

453 all pairwise comparisons within a treatment. Standard statistical tools are therefore not applicable for
454 assigning statistical significance when comparing β NTI distributions. However, as shown in Figures 4b
455 and S4b, there is an obvious shift to lower β NTI values for the putatively active community in the
456 treatments with 31 or 34 cumulative dry days.

457

458 The other aspect of the environment examined here (i.e., OM thermodynamics) also had significant
459 relationships with both microbial processes (Fig. 1, arrow 3) and properties (Fig. 1, arrow 4). More
460 specifically, respiration rates decreased significantly as a negative exponential function of increasing
461 ΔG^0_{Cox} ($R^2 = 0.34$; $p = 0.001$; Fig. 5a). This indicates a decrease in respiration rate as OM
462 thermodynamic properties shifted towards lower favorability for oxidation (i.e., larger values of ΔG^0_{Cox}).
463 Similarly, we found that the strength of deterministic assembly associated with the putatively active
464 community increased linearly with ΔG^0_{Cox} ($R^2 = 0.40$; $p = 0.001$; Fig. 5b). The relationships were clearly
465 structured by among-treatment shifts in respiration rate, β NTI, and favorability of organic matter
466 (ΔG^0_{Cox}). The strength of deterministic assembly associated with the whole community was unrelated to
467 ΔG^0_{Cox} ($p = 0.64$) (Fig. S6).

468

469 The conceptual model described in Figure 1 focuses primarily on connections among environmental
470 and/or microbial attributes, but there are potentially important relationships within attribute categories.
471 In particular, within the environmental category there is the potential for an influence of disturbance on
472 OM thermodynamics. Such an effect was found for OM thermodynamics as measured by ΔG^0_{Cox} (Fig.
473 5c). Using the same approach as for analyses described above, we combined data for treatments with 0-
474 27 cumulative dry days and compared that distribution to data combined across treatments with 31 or 34

475 cumulative dry days. A Mann-Whitney test comparing these distributions confirmed a significant
476 change in the ΔG^0_{Cox} distribution ($W = 189$, $p = < 0.001$)(Fig. S7).

477

478 The last component of the conceptual model considered here is the connection between microbial
479 processes occurring in a given location and cumulative system function that aggregates across locations
480 (Fig. 1, arrow 5). It is at the system level that the influence of biogeochemical hot spots (or hot
481 moments) can be evaluated. We conceptualized an aggregate system as the collection of replicate batch
482 reactors within a given experimental treatment. Based on this definition, we estimated control point
483 influence (CPI) as a measurement for the influence of biogeochemical hot spots. We observed a large
484 amount of variation in CPI across experimental treatments, but there was no clear, direct influence of the
485 treatments on CPI (Fig. 4). The largest value of CPI observed (> 0.9) was associated with the treatment
486 that imposed 31 cumulative dry days. This treatment also had the lowest median respiration rates across
487 all treatments (Fig. 4). We did not find any significant relationship ($p > 0.70$) between within-treatment beta-
488 dispersion of the community (whole and putatively-active) and CPI, suggesting that within-treatment beta-
489 dispersion of the community is not a better predictor of CPI.

490

491 4 Discussion

492 Mechanistic evaluation of microbe-environment interactions is fundamental to understanding microbe-
493 mediated ecosystem function. Inspired by a microbe-environment-ecosystem framework proposed by
494 Hall et al. (Hall et al., 2018) we proposed and evaluated a modified framework linking microbial
495 characteristics (membership, emergent properties, processes), the environment (disturbance, OM
496 thermodynamics), and cumulative ecosystem function (CPI) of hyporheic zone sediments. Our results

497 provide clear support for the overall conceptual framework and further point to an iterative loop among
498 OM thermodynamics, respiration rates, and microbial community assembly that can be initiated by
499 externally-imposed disturbance. Furthermore, our results indicate that the iterative thermodynamics-
500 assembly-respiration loop may be initiated through threshold-like impacts of disturbance that were
501 observed only after 31 or more cumulative days of desiccation.

502

503 We first evaluated emergent community properties as a function of microbial membership by studying
504 the relative influences of stochasticity and determinism over community assembly. Taking this

505 approach, we found fully balanced stochastic-deterministic influences over the whole community, in
506 which each contributed to 50% of the variation in community composition. The relative influences of
507 stochasticity and determinism have been quantified for many microbial systems and the estimates are
508 highly variable (Tripathi et al., 2018; Wang et al., 2013). In addition, within the deterministic
509 component of assembly, homogeneous selection had a far greater influence than variable selection.

510 Previous work has also observed a broad range of contributions from homogeneous and variable
511 selection (Fillinger et al., 2019; Graham et al., 2016; Li et al., 2019; Sengupta et al., 2019a; Whitman et
512 al., 2018). As such, the assembly-associated outcomes observed here for the whole community are not
513 unexpected relative to previous work. Very few studies, however, have examined the relative influences
514 of different assembly components over putatively active microbial communities. This focus is critical in
515 our framework since many microorganisms are inactive while the active community remains sensitive to
516 abiotic stresses and contributes to ecosystem function.

517

518 For the putatively active communities we found that across all treatments both stochasticity and
519 determinism were important, though deterministic assembly had greater influence. This deviates

520 quantitatively from the whole community in which the influences of stochasticity and determinism were
521 more balanced. The difference in assembly influences in whole- and putatively-active communities is
522 likely driven by the duration of the imposed experimental treatments (two weeks). This time period may
523 not be sufficient for birth and death events to restructure the community composition. Instead,
524 physiological responses as a function of decreases and increases in microbial activity (changes in cDNA
525 signatures) is more likely. A stronger disturbance (*e.g.*, imposing the treatments for a longer period of
526 time) may provide further insights into the impacts of disturbance on the whole community (*e.g.*, evident
527 as changes in gDNA signatures). Consistent with the whole community results, however, was the
528 dominance of homogeneous selection within the deterministic component of assembly. The strong
529 influence of homogeneous selection is likely due to selection-based constraints imposed by aspects of
530 the experimental system that did not vary across treatments. For example, mineralogy is known to
531 strongly influence microbial communities (Boyd et al., 2007; Carson et al., 2009; Doetterl et al., 2018;
532 Fauvel et al., 2019; Mauck and Roberts, 2007; Stegen et al., 2016) and was homogenized across the
533 experimental batch reactors, thereby potentially imposing homogeneous selection on both the whole and
534 putatively active communities.

535

536 Our study uniquely evaluates null-model outcomes of putatively-active community assemblies in
537 hyporheic zone sediments, where homogeneous selection was further enhanced by our experimentally
538 imposed hydrologic disturbances. Increased homogeneous selection in response to disturbance is
539 consistent with previous work in aquatic (Chase, 2007) and soil systems. For example, in a soil system,
540 disturbance led to an immediate increase in homogeneous selection for the putatively active community
541 (Jurburg et al., 2017). The strong influence of homogeneous selection on the putatively active
542 community is not always observed, however, suggesting it may be tied to acute disturbance. That is, Jia

543 et al. (2020) recently found that within a natural soil chronosequence, variable selection was stronger for
544 putatively-active communities while homogeneous selection influenced the whole community assembly.
545 Our results combined with these previous studies indicate that community assembly of putatively-active
546 members may be more closely linked to short-term environmental change than assembly of the whole
547 community.

548

549 In addition to being more sensitive to disturbance, we find that assembly of the putatively active
550 community was more strongly tied to microbial processes (i.e., respiration rate), than was the whole
551 community. A strong link between biogeochemical rates and the putatively active community is
552 consistent with previous studies (Freedman et al., 2015; Levy-Booth et al., 2019). More specifically, we
553 observed a negative relationship between respiration rate and absolute values of β NTI for the putatively
554 active community, but no relationship for the whole community. The direction of this relationship is
555 opposite to our hypothesis. While stronger selection should remove mal-adapted individuals, leading to
556 higher biogeochemical rates (Graham and Stegen, 2017), increased selection in our experiment was
557 imposed by disturbance that appeared to directly suppress respiration rates due to desiccation (Baldwin
558 and Mitchell, 2000; Manzoni et al., 2012). The simultaneous suppression of respiration and imposition
559 of stronger selection in treatments with 31 or 34 days of dry conditions (Fig. 3b) led to the negative
560 relationship between respiration and the strength of selection. The lack of such relationships when
561 considering the whole community indicates that a greater focus on assembly dynamics of putatively
562 active communities could reveal new insights into the multi-component linkages among microbes, the
563 environment, and function.

564

565 Disturbance also impacted OM thermodynamics and respiration rates, potentially initiating an iterative
566 loop among microbial assembly, microbial processes, and the abiotic environment. In this iterative loop
567 the direction of causation between OM thermodynamics and microbial processes (Fig. 1, arrow 3) is not
568 clear due to feedbacks, though we interpret a direction of causation from OM thermodynamics to
569 microbial properties in terms of community assembly (Fig. 1 arrow 4). As such, there may be a loop
570 between OM thermodynamics and microbial processes (i.e., respiration) embedded in a larger loop that
571 also includes microbial properties (i.e., community assembly). Such feedbacks are inherent in complex
572 systems and often lead to non-linear dynamics as observed here in terms of the threshold-like impact of
573 desiccation on multiple system components (Pérez Castro et al., 2019; Prosser and Martiny, 2020).

574

575 As key elements of the inferred system of feedbacks, the links among OM thermodynamic properties,
576 respiration, and desiccation found here are consistent with recent work tied to the same field system.
577 That is, Garayburu-Caruso et al. (Garayburu-Caruso et al., 2020) also showed decreasing aerobic
578 respiration with decreasing favorability for oxidation (i.e., larger values of ΔG^0_{Cox}) using sediments
579 sourced ~2 years previously from the same field system. In addition, the impacts of desiccation found
580 here are similar to Goldman et al. (Goldman et al., 2017) after re-inundation. This impact of desiccation
581 on respiration contrasts with the Birch effect (Birch and Friend, 1956) in soils whereby desiccation
582 followed by re-wetting leads to enhanced respiration. The consistency across hyporheic zone studies and
583 deviation from classical soil phenomena points to potential consistency in governing processes within
584 the hyporheic zone that deviate from processes operating in soil systems. Further evaluation is needed
585 across additional hyporheic zone systems to rigorously evaluate this inference, however.

586

587 In addition to linkages between the environment and microbial aspects of the system, our study revealed
588 connections within the environmental components of the conceptual framework. That is, greater
589 cumulative desiccation caused an increase in ΔG^0_{Cox} , indicating a significant change in OM
590 thermodynamics (Fig. 5c). While our data cannot pinpoint governing mechanism(s), we hypothesize that
591 the ΔG^0_{Cox} response may have been tied to increased ion concentration following desiccation. For
592 example, OM chemistry may have been altered due to changes in abiotic sorption, limitations of
593 microbially accessible C due to water potential constraints, and/or osmolyte production and formation of
594 extracellular polymeric substances (Fierer et al., 2003; Gionchetta et al., 2020; Homyak et al., 2018).

595

596 Irrespective of mechanisms, the shift in OM thermodynamics in response to desiccation was associated
597 with a decline in respiration. We infer a causal connection between OM thermodynamics and
598 respiration, potentially triggered by desiccation-driven shifts in OM chemistry and/or microbial
599 physiology. This causal connection is supported by recent work (Garayburu-Caruso et al., 2020) and the
600 observation of a continuous function between ΔG^0_{Cox} and respiration rate that transcended experimental
601 treatments. Desiccation therefore likely influences and may even initiate an iterative loop among OM
602 thermodynamics, microbial assembly, and biogeochemistry that underlies cumulative system function.

603

604 Cumulative system function can often be driven by ecosystem control points (Bernhardt et al., 2017),
605 but we observed relatively little indication of such behavior. That is, estimates of control point influence
606 (CPI) were relatively low across most treatments. CPI is theoretically constrained to range from 0.5-1,
607 with lower values indicating smaller influences of control points. In our study, all but one treatment had
608 CPI between ~0.5 and 0.7. The associated distributions of respiration rates did not contain obvious
609 outliers such that we interpret CPI values in the 0.5-0.7 range to be relatively low and not strongly

610 influenced by control points or biogeochemical hot spots/moments (McClain et al., 2003). The treatment
611 with 31 cumulative days of desiccation diverged from the rest in having a CPI value of ~0.9. This large
612 CPI was due to a single outlier (Fig. 5a) such that most of the cumulative respiration across reactors was
613 contributed by that single reactor. We interpret that single reactor as a biogeochemical hot spot or
614 control point within that experimental treatment. It is unclear, however, what led to such behavior as
615 disturbance did not have any systematic influence on CPI.

616

617 A strength of CPI as a metric is that it allows for direct quantitative comparisons across studies, systems,
618 and scales. Ours is the first study to estimate CPI, however, such that we cannot yet make comparisons
619 to previous work. Through future comparisons it will be possible to evaluate the strengths, weaknesses,
620 and behavior of CPI. We expect that some patterns may emerge such as CPI having a greater likelihood
621 to reach very high values (near 1) in systems with relatively low rates on average. In these conditions,
622 even a modest quantitative increase in biogeochemical rates can lead to a large proportional change such
623 that most cumulative function is from a single point in space and/or time, resulting in large CPI. We also
624 expect that some biogeochemical processes will show greater variation in CPI than others, potentially
625 due to variation in degree of functional redundancy (Louca et al., 2018). For example, processes such as
626 respiration can be performed by numerous microbial taxa (i.e., there is high functional redundancy),
627 while others are more constrained to a relatively small number of taxa (e.g., ammonia oxidation). We
628 hypothesize that CPI may be lower on average and less variable across systems and scales for
629 biogeochemical processes with greater functional redundancy. Additional work will be needed to test
630 this hypothesis.

631

632 **5 Conclusions**

633 In this study we coupled intrinsic characteristics of natural hyporheic zone sediments with imposed
634 constraints in the form of desiccation to evaluate an *a priori* conceptual framework modified from Hall
635 et al. (Hall et al., 2018). Our results demonstrated strong and often non-linear connections among
636 desiccation, OM thermodynamics, assembly of the putatively active microbial community, and
637 respiration rates. Collating our results points to further modification of the framework into an *a*
638 *posteriori* conceptual model containing nested feedback loops (Fig. 6). This conceptual model is
639 consistent with the recently proposed unification of microbial ecology around the concepts of external
640 forcing, internal dynamics, and historical contingencies (Stegen et al., 2018a). That is, we hypothesize
641 that external forcing imposed by desiccation initiates multiple internal loops that drive biological and
642 chemical dynamics that, in turn, underlie respiration responses to re-wetting that are contingent on
643 desiccation history. The development of conceptual models such as this is key to incorporating
644 additional mechanistic detail into predictive simulation models (e.g., reactive transport codes). We
645 encourage further evaluation and improvement of both our *a priori* and *a posteriori* concepts across
646 environmentally divergent conditions to generate knowledge that is transferable across systems.

647 **Code availability**

648 The R scripts used in this study are hosted on ESS-DIVE in the data package found at
649 <https://data.ess-dive.lbl.gov/view/doi:10.15485/1807580>. Null modeling scripts were based on
650 those available at https://github.com/stegen/Stegen_etal_ISME_2013.

651 **Data availability**

652 Data are available on the ESS-DIVE archive at the following link [https://data.ess-
653 dive.lbl.gov/view/doi:10.15485/1807580](https://data.ess-dive.lbl.gov/view/doi:10.15485/1807580). Sequence data is available on NCBI's Sequence Read
654 Archive PRJNA641165.

655 **Supplement**

656 The supplement related to this article is available online at: XXX

657 **Author contributions**

658 JCS and SF conceptualized and designed the study; JT, JW, LR, RC, SF, and VAG-C performed
659 the experiment; AS, JCS, RED, and SF analyzed data; AS, JCS, and SF drafted the manuscript
660 and all authors contributed to further writing.

661 **Competing interests**

662 The authors declare that they have no conflict of interest.

663 **Acknowledgements**

664 We thank Amy Goldman and Nathan Johnson for developing graphics. The initial experimental stages
665 of this work were supported by the PREMIS Initiative at the Pacific Northwest National Laboratory
666 (PNNL) with funding from the Laboratory Directed Research and Development Program at PNNL, a
667 multi-program national laboratory operated by Battelle for the US Department of Energy under Contract
668 DE-AC05-76RL01830. The later stages of this work (e.g., data analysis, conceptual interpretation,
669 manuscript development) were supported by the U.S. Department of Energy-BER program, as part of an
670 Early Career Award to JCS at PNNL. A portion of the research was performed using EMSL, a DOE
671 Office of Science User Facility sponsored by the Office of Biological and Environmental Research.

672

673 **References**

674 Arntzen, E.: Effects of fluctuating river flow on groundwater/surface water mixing in the hyporheic zone
675 of a regulated, large cobble bed river - Arntzen - 2006 - River Research and Applications - Wiley Online
676 Library, <https://onlinelibrary.wiley.com/doi/abs/10.1002/rra.947>, last access: 8 July 2020, 2006.

677

678 Arora, B., Briggs, M. A., Zarnetske, J., Stegen, J. C., Gomez-Velez, J., Dwivedi, D. and Steefel, C. I.:
679 Hot Spots and Hot Moments in the Critical Zone: Identification of and Incorporation into Reactive
680 Transport Models, in Biogeochemistry of the Critical Zone, edited by A. Wymore, W. Yang, W. Silver,
681 B. McDowell, and J. Chorover, Springer-Nature, , 2020.

682

683 Baldwin, D. S. and Mitchell, A. M.: The effects of drying and re-flooding on the sediment and soil
684 nutrient dynamics of lowland river–floodplain systems: a synthesis, *Regul. Rivers Res. Manag.*, 16(5),
685 457–467, [https://doi.org/10.1002/1099-1646\(200009/10\)16:5<457::AID-RRR597>3.0.CO;2-B](https://doi.org/10.1002/1099-1646(200009/10)16:5<457::AID-RRR597>3.0.CO;2-B), 2000.

686

687 Barnard, R. L., Osborne, C. A. and Firestone, M. K.: Changing precipitation pattern alters soil microbial
688 community response to wet-up under a Mediterranean-type climate, *ISME J.*, 9(4), 946–957,
689 <https://doi.org/10.1038/ismej.2014.192>, 2015.

690

691 Bartelme, R. P., Custer, J. M., Dupont, C. L., Espinoza, J. L., Torralba, M., Khalili, B. and Carini, P.:
692 Influence of Substrate Concentration on the Culturability of Heterotrophic Soil Microbes Isolated by
693 High-Throughput Dilution-to-Extinction Cultivation, *mSphere*, 5(1),
694 <https://doi.org/10.1128/mSphere.00024-20>, 2020.

695

696 Behrens, S., Kappler, A. and Obst, M.: Linking environmental processes to the in situ functioning of
697 microorganisms by high-resolution secondary ion mass spectrometry (NanoSIMS) and scanning
698 transmission X-ray microscopy (STXM), *Environ. Microbiol.*, 14(11), 2851–2869,
699 <https://doi.org/10.1111/j.1462-2920.2012.02724.x>, 2012.

700

701 Bernhardt, E. S., Blaszcak, J. R., Ficken, C. D., Fork, M. L., Kaiser, K. E. and Seybold, E. C.: Control
702 Points in Ecosystems: Moving Beyond the Hot Spot Hot Moment Concept, *Ecosystems*, 20(4), 665–682,
703 <https://doi.org/10.1007/s10021-016-0103-y>, 2017.

704

705 Bier, R. L., Bernhardt, E. S., Boot, C. M., Graham, E. B., Hall, E. K., Lennon, J. T., Nemergut, D. R.,
706 Osborne, B. B., Ruiz-González, C., Schimel, J. P., Waldrop, M. P. and Wallenstein, M. D.: Linking
707 microbial community structure and microbial processes: an empirical and conceptual overview, *FEMS
708 Microbiol. Ecol.*, 91(10), <https://doi.org/10.1093/femsec/fiv113>, 2015.

709

710 Birch, H. F.: Mineralisation of plant nitrogen following alternate wet and dry conditions, *Plant Soil*,
711 20(1), 43–49, <https://doi.org/10.1007/BF01378096>, 1964.

712

713 Birch, H. F. and Friend, M. T.: Humus Decomposition in East African Soils, *Nature*, 178(4531), 500–
714 501, <https://doi.org/10.1038/178500a0>, 1956.

715

716 Blazewicz, S. J., Barnard, R. L., Daly, R. A. and Firestone, M. K.: Evaluating rRNA as an indicator of

717 microbial activity in environmental communities: limitations and uses, ISME J., 7(11), 2061–2068,
718 <https://doi.org/10.1038/ismej.2013.102>, 2013.

719

720 Boano, F., Harvey, J. W., Marion, A., Packman, A. I., Revelli, R., Ridolfi, L. and Wörman, A.:
721 Hyporheic flow and transport processes: Mechanisms, models, and biogeochemical implications, Rev.
722 Geophys., 52(4), 603–679, <https://doi.org/10.1002/2012RG000417>, 2014.

723

724 Bottos, E. M., Kennedy, D. W., Romero, E. B., Fansler, S. J., Brown, J. M., Bramer, L. M., Chu, R. K.,
725 Tfaily, M. M., Jansson, J. K. and Stegen, J. C.: Dispersal limitation and thermodynamic constraints
726 govern spatial structure of permafrost microbial communities, FEMS Microbiol. Ecol., 94(8),
727 <https://doi.org/10.1093/femsec/fiy110>, 2018.

728

729 Boyd, E. S., Cummings, D. E. and Geesey, G. G.: Mineralogy Influences Structure and Diversity of
730 Bacterial Communities Associated with Geological Substrata in a Pristine Aquifer, Microb. Ecol., 54(1),
731 170–182, <https://doi.org/10.1007/s00248-006-9187-9>, 2007.

732

733 Boye, K., Noël, V., Tfaily, M. M., Bone, S. E., Williams, K. H., Bargar, J. R. and Fendorf, S.:
734 Thermodynamically controlled preservation of organic carbon in floodplains, Nat. Geosci., 10(6), 415–
735 419, <https://doi.org/10.1038/ngeo2940>, 2017.

736

737 Brown, J., Zavoshy, N., Brisbaw, C. J. and McCue, L. A.: Hundo: a Snakemake workflow for microbial
738 community sequence data, PeerJ Inc., 2018.

739

740 Burrows, R. M., Rutledge, H., Bond, N. R., Eberhard, S. M., Auhl, A., Andersen, M. S., Valdez, D. G.
741 and Kennard, M. J.: High rates of organic carbon processing in the hyporheic zone of intermittent
742 streams, Sci. Rep., 7(1), 1–11, <https://doi.org/10.1038/s41598-017-12957-5>, 2017.

743

744 Caporaso, J. G.: EMP 16S Illumina Amplicon Protocol, ,
745 <https://doi.org/10.17504/protocols.io.nuudeww>, 2018.

746

747 Cardoso, D. C., Sandionigi, A., Cretoiu, M. S., Casiraghi, M., Stal, L. and Bolhuis, H.: Comparison of
748 the active and resident community of a coastal microbial mat, Sci. Rep., 7(1), 1–10,
749 <https://doi.org/10.1038/s41598-017-03095-z>, 2017.

750

751 Carson, J. K., Campbell, L., Rooney, D., Clipson, N. and Gleeson, D. B.: Minerals in soil select distinct
752 bacterial communities in their microhabitats, FEMS Microbiol. Ecol., 67(3), 381–388,
753 <https://doi.org/10.1111/j.1574-6941.2008.00645.x>, 2009.

754

755 Chase, J. M.: Drought mediates the importance of stochastic community assembly, PNAS, 104,
756 17430–17434, <https://doi.org/10.1073/pnas.0704350104>, 2007.

757

758 Chen, W., Ren, K., Isabwe, A., Chen, H., Liu, M. and Yang, J.: Stochastic processes shape
759 microeukaryotic community assembly in a subtropical river across wet and dry seasons, Microbiome,
760 7(1), 138, <https://doi.org/10.1186/s40168-019-0749-8>, 2019.

761

762 Daly, R. A., Borton, M. A., Wilkins, M. J., Hoyt, D. W., Kountz, D. J., Wolfe, R. A., Welch, S. A.,

763 Marcus, D. N., Trexler, R. V., MacRae, J. D., Krzycki, J. A., Cole, D. R., Mouser, P. J. and Wrighton,
764 K. C.: Microbial metabolisms in a 2.5-km-deep ecosystem created by hydraulic fracturing in shales, *Nat.*
765 *Microbiol.*, 1(10), 1–9, <https://doi.org/10.1038/nmicrobiol.2016.146>, 2016.

766

767 Danczak, R. E., Goldman, A. E., Chu, R. K., Toyoda, J. G., Garayburu-Caruso, V. A., Tolić, N.,
768 Graham, E. B., Morad, J. W., Renteria, L., Wells, J. R., Herzog, S. P., Ward, A. S. and Stegen, J. C.:
769 Ecological theory applied to environmental metabolomes reveals compositional divergence despite
770 conserved molecular properties, *bioRxiv*, 2020.02.12.946459,
771 <https://doi.org/10.1101/2020.02.12.946459>, 2020.

772

773 Demars, B. O. L.: Hydrological pulses and burning of dissolved organic carbon by stream respiration,
774 *Limnol. Oceanogr.*, 64(1), 406–421, <https://doi.org/10.1002/lno.11048>, 2019.

775

776 Dini-Andreote, F., Stegen, J. C., Elsas, J. D. van and Salles, J. F.: Disentangling mechanisms that
777 mediate the balance between stochastic and deterministic processes in microbial succession, *Proc. Natl.*
778 *Acad. Sci.*, 112(11), E1326–E1332, <https://doi.org/10.1073/pnas.1414261112>, 2015.

779

780 Doetterl, S., Berhe, A. A., Arnold, C., Bodé, S., Fiener, P., Finke, P., Fuchslueger, L., Griepentrog, M.,
781 Harden, J. W., Nadeu, E., Schnecker, J., Six, J., Trumbore, S., Van Oost, K., Vogel, C. and Boeckx, P.:
782 Links among warming, carbon and microbial dynamics mediated by soil mineral weathering, *Nat.*
783 *Geosci.*, 11(8), 589–593, <https://doi.org/10.1038/s41561-018-0168-7>, 2018.

784

785 Fatichi, S., Manzoni, S., Or, D. and Paschalis, A.: A Mechanistic Model of Microbially Mediated Soil
786 Biogeochemical Processes: A Reality Check, *Glob. Biogeochem. Cycles*, 33(6), 620–648,
787 <https://doi.org/10.1029/2018GB006077>, 2019.

788

789 Fauvel, B., Cauchie, H.-M., Gantzer, C. and Ogorzaly, L.: Influence of physico-chemical characteristics
790 of sediment on the in situ spatial distribution of F-specific RNA phages in the riverbed, *FEMS*
791 *Microbiol. Ecol.*, 95(2), <https://doi.org/10.1093/femsec/fiy240>, 2019.

792

793 Feng, Y., Chen, R., Stegen, J. C., Guo, Z., Zhang, J., Li, Z. and Lin, X.: Two key features influencing
794 community assembly processes at regional scale: Initial state and degree of change in environmental
795 conditions, *Mol. Ecol.*, 27(24), 5238–5251, <https://doi.org/10.1111/mec.14914>, 2018.

796

797 Fierer, N., Allen, A. S., Schimel, J. P. and Holden, P. A.: Controls on microbial CO₂ production: a
798 comparison of surface and subsurface soil horizons, *Glob. Change Biol.*, 9(9), 1322–1332,
799 <https://doi.org/10.1046/j.1365-2486.2003.00663.x>, 2003.

800

801 Fillinger, L., Zhou, Y., Kellermann, C. and Griebler, C.: Non-random processes determine the
802 colonization of groundwater sediments by microbial communities in a pristine porous aquifer, *Environ.*
803 *Microbiol.*, 21(1), 327–342, <https://doi.org/10.1111/1462-2920.14463>, 2019.

804

805 Fischer, H., Kloep, F., Wilzcek, S. and Pusch, M. T.: A River’s Liver – Microbial Processes within the
806 Hyporheic Zone of a Large Lowland River, *Biogeochemistry*, 76(2), 349–371,
807 <https://doi.org/10.1007/s10533-005-6896-y>, 2005.

808

809 Freedman, Z. B., Romanowicz, K. J., Upchurch, R. A. and Zak, D. R.: Differential responses of total
810 and active soil microbial communities to long-term experimental N deposition, *Soil Biol. Biochem.*, 90,
811 275–282, <https://doi.org/10.1016/j.soilbio.2015.08.014>, 2015.

812

813 Fu, X., Li, Y., Meng, Y., Yuan, Q., Zhang, Z., Norbäck, D., Deng, Y., Zhang, X. and Sun, Y.: Derived
814 ecological niches of indoor microbes are crucial for asthma symptoms in university dormitories,
815 *bioRxiv*, 2020.01.05.893529, <https://doi.org/10.1101/2020.01.05.893529>, 2020.

816

817 Garayburu-Caruso, V. A., Stegen, J. C., Song, H.-S., Renteria, L., Wells, J., Garcia, W., Resch, C. T.,
818 Goldman, A. E., Chu, R. K., Toyoda, J. and Graham, E. B.: Carbon Limitation Leads to Thermodynamic
819 Regulation of Aerobic Metabolism, *Environ. Sci. Technol. Lett.*,
820 <https://doi.org/10.1021/acs.estlett.0c00258>, 2020.

821

822 Gilbert, J. A., Jansson, J. K. and Knight, R.: Earth Microbiome Project and Global Systems Biology,
823 *mSystems*, 3(3), <https://doi.org/10.1128/mSystems.00217-17>, 2018.

824

825 Gionchetta, G., Oliva, F., Romani, A. M. and Baneras, L.: Hydrological variations shape diversity and
826 functional responses of streambed microbes, *Sci. Total Environ.*, 714, 136838,
827 <https://doi.org/10.1016/j.scitotenv.2020.136838>, 2020.

828

829 Goldman, A. E., Graham, E. B., Crump, A. R., Kennedy, D. W., Romero, E. B., Anderson, C. G., Dana,
830 K. L., Resch, C. T., Fredrickson, J. K. and Stegen, J. C.: Biogeochemical cycling at the aquatic–
831 terrestrial interface is linked to parafluvial hyporheic zone inundation history, *Biogeosciences*, 14(18),
832 4229–4241, <https://doi.org/10.5194/bg-14-4229-2017>, 2017.

833

834 Graham, E. B. and Stegen, J. C.: Dispersal-Based Microbial Community Assembly Decreases
835 Biogeochemical Function, *Processes*, 5(4), 65, <https://doi.org/10.3390/pr5040065>, 2017.

836

837 Graham, E. B., Crump, A. R., Resch, C. T., Fansler, S., Arntzen, E., Kennedy, D. W., Fredrickson, J. K.
838 and Stegen, J. C.: Coupling Spatiotemporal Community Assembly Processes to Changes in Microbial
839 Metabolism, *Front. Microbiol.*, 7, <https://doi.org/10.3389/fmicb.2016.01949>, 2016.

840

841 Graham, E. B., Tfaily, M. M., Crump, A. R., Goldman, A. E., Bramer, L. M., Arntzen, E., Romero, E.,
842 Resch, C. T., Kennedy, D. W. and Stegen, J. C.: Carbon Inputs From Riparian Vegetation Limit
843 Oxidation of Physically Bound Organic Carbon Via Biochemical and Thermodynamic Processes, *J.*
844 *Geophys. Res. Biogeosciences*, 122(12), 3188–3205, <https://doi.org/10.1002/2017JG003967>, 2017a.

845

846 Graham, E. B., Crump, A. R., Resch, C. T., Fansler, S., Arntzen, E., Kennedy, D. W., Fredrickson, J. K.
847 and Stegen, J. C.: Deterministic influences exceed dispersal effects on hydrologically-connected
848 microbiomes, *Environ. Microbiol.*, 19(4), 1552–1567, <https://doi.org/10.1111/1462-2920.13720>, 2017b.

849

850 Graham, E. B., Crump, A. R., Kennedy, D. W., Arntzen, E., Fansler, S., Purvine, S. O., Nicora, C. D.,
851 Nelson, W., Tfaily, M. M. and Stegen, J. C.: Multi 'omics comparison reveals metabolome
852 biochemistry, not microbiome composition or gene expression, corresponds to elevated biogeochemical
853 function in the hyporheic zone, *Sci. Total Environ.*, 642, 742–753,
854 <https://doi.org/10.1016/j.scitotenv.2018.05.256>, 2018.

855
856 Grilli, J., Barabás, G., Michalska-Smith, M. J. and Allesina, S.: Higher-order interactions stabilize
857 dynamics in competitive network models, *Nature*, 548(7666), 210–213,
858 <https://doi.org/10.1038/nature23273>, 2017.

859
860 Hall, E. K., Bernhardt, E. S., Bier, R. L., Bradford, M. A., Boot, C. M., Cotner, J. B., del Giorgio, P. A.,
861 Evans, S. E., Graham, E. B., Jones, S. E., Lennon, J. T., Locey, K. J., Nemergut, D., Osborne, B. B.,
862 Rocca, J. D., Schimel, J. P., Waldrop, M. P. and Wallenstein, M. D.: Understanding how microbiomes
863 influence the systems they inhabit, *Nat. Microbiol.*, 3(9), 977–982, <https://doi.org/10.1038/s41564-018-0201-z>, 2018.

864
865 Homyak, P. M., Blankinship, J. C., Slessarev, E. W., Schaeffer, S. M., Manzoni, S. and Schimel, J. P.:
866 Effects of altered dry season length and plant inputs on soluble soil carbon, *Ecology*, 99(10), 2348–
867 2362, <https://doi.org/10.1002/ecy.2473>, 2018.

868
869
870 Jia, X., Dini-Andreote, F. and Falcão Salles, J.: Comparing the Influence of Assembly Processes
871 Governing Bacterial Community Succession Based on DNA and RNA Data, *Microorganisms*, 8(6), 798,
872 <https://doi.org/10.3390/microorganisms8060798>, 2020.

873
874 Jurburg, S. D., Nunes, I., Stegen, J. C., Le Roux, X., Priemé, A., Sørensen, S. J. and Salles, J. F.:
875 Autogenic succession and deterministic recovery following disturbance in soil bacterial communities,
876 *Sci. Rep.*, 7(1), 1–11, <https://doi.org/10.1038/srep45691>, 2017.

877
878 Kaufman, M. H., Cardenas, M. B., Buttles, J., Kessler, A. J. and Cook, P. L. M.: Hyporheic hot
879 moments: Dissolved oxygen dynamics in the hyporheic zone in response to surface flow perturbations,
880 *Water Resour. Res.*, 53(8), 6642–6662, <https://doi.org/10.1002/2016WR020296>, 2017.

881
882 Kearns, P. J., Angell, J. H., Howard, E. M., Deegan, L. A., Stanley, R. H. R. and Bowen, J. L.: Nutrient
883 enrichment induces dormancy and decreases diversity of active bacteria in salt marsh sediments, *Nat.*
884 *Commun.*, 7(1), 12881, <https://doi.org/10.1038/ncomms12881>, 2016.

885
886 König, S., Worrich, A., Banitz, T., Centler, F., Harms, H., Kästner, M., Miltner, A., Wick, L. Y.,
887 Thullner, M. and Frank, K.: Spatiotemporal disturbance characteristics determine functional stability
888 and collapse risk of simulated microbial ecosystems, *Sci. Rep.*, 8(1), 1–13,
889 <https://doi.org/10.1038/s41598-018-27785-4>, 2018.

890
891 Larned, S. T., Datry, T., Arscott, D. B. and Tockner, K.: Emerging concepts in temporary-river ecology,
892 *Freshw. Biol.*, 55(4), 717–738, <https://doi.org/10.1111/j.1365-2427.2009.02322.x>, 2010.

893
894 LaRowe, D. E. and Van Cappellen, P.: Degradation of natural organic matter: A thermodynamic
895 analysis, *Geochim. Cosmochim. Acta*, 75(8), 2030–2042, <https://doi.org/10.1016/j.gca.2011.01.020>,
896 2011.

897
898 Leventhal, G. E., Ackermann, M. and Schiessl, K. T.: Why microbes secrete molecules to modify their
899 environment: the case of iron-chelating siderophores, *J. R. Soc. Interface*, 16(150), 20180674,
900 <https://doi.org/10.1098/rsif.2018.0674>, 2019.

901 Levy-Booth, D. J., Giesbrecht, I. J. W., Kellogg, C. T. E., Heger, T. J., D'Amore, D. V., Keeling, P. J.,
902 Hallam, S. J. and Mohn, W. W.: Seasonal and ecohydrological regulation of active microbial
903 populations involved in DOC, CO₂, and CH₄ fluxes in temperate rainforest soil, *ISME J.*, 13(4), 950–
904 963, <https://doi.org/10.1038/s41396-018-0334-3>, 2019.

905

906 Li, Y., Gao, Y., Zhang, W., Wang, C., Wang, P., Niu, L. and Wu, H.: Homogeneous selection dominates
907 the microbial community assembly in the sediment of the Three Gorges Reservoir, *Sci. Total Environ.*,
908 690, 50–60, <https://doi.org/10.1016/j.scitotenv.2019.07.014>, 2019.

909

910 Lloyd-Price, J., Arze, C., Ananthakrishnan, A. N., Schirmer, M., Avila-Pacheco, J., Poon, T. W.,
911 Andrews, E., Ajami, N. J., Bonham, K. S., Brislawn, C. J., Casero, D., Courtney, H., Gonzalez, A.,
912 Graeber, T. G., Hall, A. B., Lake, K., Landers, C. J., Mallick, H., Plichta, D. R., Prasad, M., Rahnavard,
913 G., Sauk, J., Shungin, D., Vázquez-Baeza, Y., White, R. A., Braun, J., Denson, L. A., Jansson, J. K.,
914 Knight, R., Kugathasan, S., McGovern, D. P. B., Petrosino, J. F., Stappenbeck, T. S., Winter, H. S.,
915 Clish, C. B., Franzosa, E. A., Vlamakis, H., Xavier, R. J. and Huttenhower, C.: Multi-omics of the gut
916 microbial ecosystem in inflammatory bowel diseases, *Nature*, 569(7758), 655–662,
917 <https://doi.org/10.1038/s41586-019-1237-9>, 2019.

918

919 Louca, S., Polz, M. F., Mazel, F., Albright, M. B. N., Huber, J. A., O'Connor, M. I., Ackermann, M.,
920 Hahn, A. S., Srivastava, D. S., Crowe, S. A., Doebeli, M. and Parfrey, L. W.: Function and functional
921 redundancy in microbial systems, *Nat. Ecol. Evol.*, 2(6), 936–943, <https://doi.org/10.1038/s41559-018-0519-1>, 2018.

922

923

924 Malik, A. A., Martiny, J. B. H., Brodie, E. L., Martiny, A. C., Treseder, K. K. and Allison, S. D.:
925 Defining trait-based microbial strategies with consequences for soil carbon cycling under climate
926 change, *ISME J.*, 14(1), 1–9, <https://doi.org/10.1038/s41396-019-0510-0>, 2020.

927

928 Manzella, M., Geiss, R. and Hall, E. K.: Evaluating the stoichiometric trait distributions of cultured
929 bacterial populations and uncultured microbial communities, *Environ. Microbiol.*, 21(10), 3613–3626,
930 <https://doi.org/10.1111/1462-2920.14684>, 2019.

931

932 Manzoni, S., Schimel, J. P. and Porporato, A.: Responses of soil microbial communities to water stress:
933 results from a meta-analysis, *Ecology*, 93(4), 930–938, <https://doi.org/10.1890/11-0026.1>, 2012.

934

935 Martínez, I., Stegen, J. C., Maldonado-Gómez, M. X., Eren, A. M., Siba, P. M., Greenhill, A. R. and
936 Walter, J.: The Gut Microbiota of Rural Papua New Guineans: Composition, Diversity Patterns, and
937 Ecological Processes, *Cell Rep.*, 11(4), 527–538, <https://doi.org/10.1016/j.celrep.2015.03.049>, 2015.

938

939 Mauck, B. S. and Roberts, J. A.: Mineralogic Control on Abundance and Diversity of Surface-Adherent
940 Microbial Communities, *Geomicrobiol. J.*, 24(3–4), 167–177,
941 <https://doi.org/10.1080/01490450701457162>, 2007.

942

943 McClain, M. E., Boyer, E. W., Dent, C. L., Gergel, S. E., Grimm, N. B., Groffman, P. M., Hart, S. C.,
944 Harvey, J. W., Johnston, C. A., Mayorga, E., McDowell, W. H. and Pinay, G.: Biogeochemical Hot
945 Spots and Hot Moments at the Interface of Terrestrial and Aquatic Ecosystems, *Ecosystems*, 6(4), 301–
946 312, <https://doi.org/10.1007/s10021-003-0161-9>, 2003.

947
948 Norland, S., Fagerbakke, K. M. and Heldal, M.: Light element analysis of individual bacteria by x-ray
949 microanalysis., *Appl. Environ. Microbiol.*, 61(4), 1357–1362, <https://doi.org/10.1128/AEM.61.4.1357-1362.1995>, 1995.

951
952 Ofițeru, I. D., Lunn, M., Curtis, T. P., Wells, G. F., Criddle, C. S., Francis, C. A. and Sloan, W. T.:
953 Combined niche and neutral effects in a microbial wastewater treatment community, *Proc. Natl. Acad.
954 Sci.*, 107(35), 15345–15350, <https://doi.org/10.1073/pnas.1000604107>, 2010.

955
956 Pérez Castro, S., Cleland, E. E., Wagner, R., Sawad, R. A. and Lipson, D. A.: Soil microbial responses
957 to drought and exotic plants shift carbon metabolism, *ISME J.*, 13(7), 1776–1787,
958 <https://doi.org/10.1038/s41396-019-0389-9>, 2019.

959
960 Prosser, J. I. and Martiny, J. B. H.: Conceptual challenges in microbial community ecology, *Philos.
961 Trans. R. Soc. B Biol. Sci.*, 375(1798), 20190241, <https://doi.org/10.1098/rstb.2019.0241>, 2020.

962 Ratzke, C., Denk, J. and Gore, J.: Ecological suicide in microbes, *Nat. Ecol. Evol.*, 2(5), 867–872,
963 <https://doi.org/10.1038/s41559-018-0535-1>, 2018.

964
965 Romaní, A. M., Vázquez, E. and Butturini, A.: Microbial Availability and Size Fractionation of
966 Dissolved Organic Carbon After Drought in an Intermittent Stream: Biogeochemical Link Across the
967 Stream–Riparian Interface, *Microb. Ecol.*, 52(3), 501–512, <https://doi.org/10.1007/s00248-006-9112-2>,
968 2006.

969
970 Sengupta, A., Stegen, J. C., Neto, A. A. M., Wang, Y., Neilson, J. W., Tatarin, T., Hunt, E., Dontsova,
971 K., Chorover, J., Troch, P. A. and Maier, R. M.: Assessing Microbial Community Patterns During
972 Incipient Soil Formation From Basalt, *J. Geophys. Res. Biogeosciences*, 124(4), 941–958,
973 <https://doi.org/10.1029/2017JG004315>, 2019a.

974
975 Sengupta, A., Indivero, J., Gunn, C., Tfaily, M. M., Chu, R. K., Toyoda, J., Bailey, V. L., Ward, N. D.
976 and Stegen, J. C.: Spatial gradients in the characteristics of soil-carbon fractions are associated with
977 abiotic features but not microbial communities, *Biogeosciences*, 16(19), 3911–3928,
978 <https://doi.org/10.5194/bg-16-3911-2019>, 2019b.

979
980 Shu, D., Guo, J., Zhang, B., He, Y. and Wei, G.: rDNA- and rRNA-derived communities present
981 divergent assemblage patterns and functional traits throughout full-scale landfill leachate treatment
982 process trains, *Sci. Total Environ.*, 646, 1069–1079, <https://doi.org/10.1016/j.scitotenv.2018.07.388>,
983 2019.

984
985 Slater, L. D., Ntarlagiannis, D., Day-Lewis, F. D., Mwakanyamale, K., Versteeg, R. J., Ward, A.,
986 Strickland, C., Johnson, C. D. and Lane, J. W.: Use of electrical imaging and distributed temperature
987 sensing methods to characterize surface water–groundwater exchange regulating uranium transport at
988 the Hanford 300 Area, Washington, *Water Resour. Res.*, 46(10),
989 <https://doi.org/10.1029/2010WR009110>, 2010.

990
991 Song, H.-S., Stegen, J. C., Graham, E. B., Lee, J.-Y., Garayburu-Caruso, V. A., Nelson, W. C., Chen,
992 X., Moulton, J. D. and Scheibe, T. D.: Representing Organic Matter Thermodynamics in

993 Biogeochemical Reactions via Substrate-Explicit Modeling, bioRxiv, 2020.02.27.968669,
994 <https://doi.org/10.1101/2020.02.27.968669>, 2020.

995

996 Starnawski, P., Bataillon, T., Ettema, T. J. G., Jochum, L. M., Schreiber, L., Chen, X., Lever, M. A.,
997 Polz, M. F., Jørgensen, B. B., Schramm, A. and Kjeldsen, K. U.: Microbial community assembly and
998 evolution in subseafloor sediment, *Proc. Natl. Acad. Sci.*, 114(11), 2940–2945,
999 <https://doi.org/10.1073/pnas.1614190114>, 2017.

1000

1001 Stegen, J. C., Lin, X., Konopka, A. E. and Fredrickson, J. K.: Stochastic and deterministic assembly
1002 processes in subsurface microbial communities, *ISME J.*, 6(9), 1653–1664,
1003 <https://doi.org/10.1038/ismej.2012.22>, 2012.

1004

1005 Stegen, J. C., Lin, X., Fredrickson, J. K., Chen, X., Kennedy, D. W., Murray, C. J., Rockhold, M. L. and
1006 Konopka, A.: Quantifying community assembly processes and identifying features that impose them,
1007 *ISME J.*, 7(11), 2069–2079, <https://doi.org/10.1038/ismej.2013.93>, 2013.

1008

1009 Stegen, J. C., Lin, X., Fredrickson, J. K. and Konopka, A. E.: Estimating and mapping ecological
1010 processes influencing microbial community assembly, *Front. Microbiol.*, 6,
1011 <https://doi.org/10.3389/fmicb.2015.00370>, 2015.

1012

1013 Stegen, J. C., Konopka, A., McKinley, J. P., Murray, C., Lin, X., Miller, M. D., Kennedy, D. W., Miller,
1014 E. A., Resch, C. T. and Fredrickson, J. K.: Coupling among Microbial Communities, *Biogeochemistry*
1015 and Mineralogy across Biogeochemical Facies, *Sci. Rep.*, 6(1), 1–14, <https://doi.org/10.1038/srep30553>,
1016 2016.

1017

1018 Stegen, J. C., Bottos, E. M. and Jansson, J. K.: A unified conceptual framework for prediction and
1019 control of microbiomes., *Curr. Opin. Microbiol.*, <https://doi.org/10.1016/j.mib.2018.06.002>, 2018a.

1020

1021 Stegen, J. C., Johnson, T., Fredrickson, J. K., Wilkins, M. J., Konopka, A. E., Nelson, W. C., Arntzen,
1022 E. V., Chrisler, W. B., Chu, R. K., Fansler, S. J., Graham, E. B., Kennedy, D. W., Resch, C. T., Tfaily,
1023 M. and Zachara, J.: Influences of organic carbon speciation on hyporheic corridor biogeochemistry and
1024 microbial ecology, *Nat. Commun.*, 9(1), 1–11, <https://doi.org/10.1038/s41467-018-02922-9>, 2018b.

1025

1026 Thompson, L. R., Sanders, J. G., McDonald, D., Amir, A., Ladau, J., Locey, K. J., Prill, R. J., Tripathi,
1027 A., Gibbons, S. M., Ackermann, G., Navas-Molina, J. A., Janssen, S., Kopylova, E., Vázquez-Baeza, Y.,
1028 González, A., Morton, J. T., Mirarab, S., Zech Xu, Z., Jiang, L., Haroon, M. F., Kanbar, J., Zhu, Q., Jin
1029 Song, S., Koscioletk, T., Bokulich, N. A., Lefler, J., Brislawn, C. J., Humphrey, G., Owens, S. M.,
1030 Hampton-Marcell, J., Berg-Lyons, D., McKenzie, V., Fierer, N., Fuhrman, J. A., Clauzet, A., Stevens,
1031 R. L., Shade, A., Pollard, K. S., Goodwin, K. D., Jansson, J. K., Gilbert, J. A. and Knight, R.: A
1032 communal catalogue reveals Earth's multiscale microbial diversity, *Nature*, 551(7681), 457–463,
1033 <https://doi.org/10.1038/nature24621>, 2017.

1034

1035 Tripathi, B. M., Stegen, J. C., Kim, M., Dong, K., Adams, J. M. and Lee, Y. K.: Soil pH mediates the
1036 balance between stochastic and deterministic assembly of bacteria, *ISME J.*, 12(4), 1072–1083,
1037 <https://doi.org/10.1038/s41396-018-0082-4>, 2018.

1038

1039 Wagner, M.: Single-cell ecophysiology of microbes as revealed by Raman microspectroscopy or
1040 secondary ion mass spectrometry imaging, *Annu. Rev. Microbiol.*, 63, 411–429,
1041 <https://doi.org/10.1146/annurev.micro.091208.073233>, 2009.

1042

1043 Wallenstein, M. D. and Hall, E. K.: A trait-based framework for predicting when and where microbial
1044 adaptation to climate change will affect ecosystem functioning, *Biogeochemistry*, 109(1), 35–47,
1045 <https://doi.org/10.1007/s10533-011-9641-8>, 2012.

1046

1047 Wang, J., Shen, J., Wu, Y., Tu, C., Soininen, J., Stegen, J. C., He, J., Liu, X., Zhang, L. and Zhang, E.:
1048 Phylogenetic beta diversity in bacterial assemblages across ecosystems: deterministic versus stochastic
1049 processes, *ISME J.*, 7(7), 1310–1321, <https://doi.org/10.1038/ismej.2013.30>, 2013.

1050

1051 Whitman, T., Neurath, R., Perera, A., Chu-Jacoby, I., Ning, D., Zhou, J., Nico, P., Pett-Ridge, J. and
1052 Firestone, M.: Microbial community assembly differs across minerals in a rhizosphere microcosm,
1053 *Environ. Microbiol.*, 20(12), 4444–4460, <https://doi.org/10.1111/1462-2920.14366>, 2018.

1054

1055 Wieder, W. R., Allison, S. D., Davidson, E. A., Georgiou, K., Hararuk, O., He, Y., Hopkins, F., Luo, Y.,
1056 Smith, M. J., Sulman, B., Todd-Brown, K., Wang, Y.-P., Xia, J. and Xu, X.: Explicitly representing soil
1057 microbial processes in Earth system models, *Glob. Biogeochem. Cycles*, 29(10), 1782–1800,
1058 <https://doi.org/10.1002/2015GB005188>, 2015.

1059

1060 Wisnoski, N. I., Muscarella, M. E., Larsen, M. L., Peralta, A. L. and Lennon, J. T.: Metabolic insight
1061 into bacterial community assembly across ecosystem boundaries, *Ecology*, 101(4), e02968,
1062 <https://doi.org/10.1002/ecy.2968>, 2020.

1063

1064 Wu, W., Lu, H.-P., Sastri, A., Yeh, Y.-C., Gong, G.-C., Chou, W.-C. and Hsieh, C.-H.: Contrasting the
1065 relative importance of species sorting and dispersal limitation in shaping marine bacterial versus protist
1066 communities, *ISME J.*, 12(2), 485–494, <https://doi.org/10.1038/ismej.2017.183>, 2018.

1067

1068 Zachara, J. M., Long, P. E., Bargar, J., Davis, J. A., Fox, P., Fredrickson, J. K., Freshley, M. D.,
1069 Konopka, A. E., Liu, C., McKinley, J. P., Rockhold, M. L., Williams, K. H. and Yabusaki, S. B.:
1070 Persistence of uranium groundwater plumes: Contrasting mechanisms at two DOE sites in the
1071 groundwater–river interaction zone, *J. Contam. Hydrol.*, 147, 45–72,
1072 <https://doi.org/10.1016/j.jconhyd.2013.02.001>, 2013.

1073

1074 Zhou, J. and Ning, D.: Stochastic Community Assembly: Does It Matter in Microbial Ecology?,
1075 *Microbiol. Mol. Biol. Rev.*, 81(4), <https://doi.org/10.1128/MMBR.00002-17>, 2017.

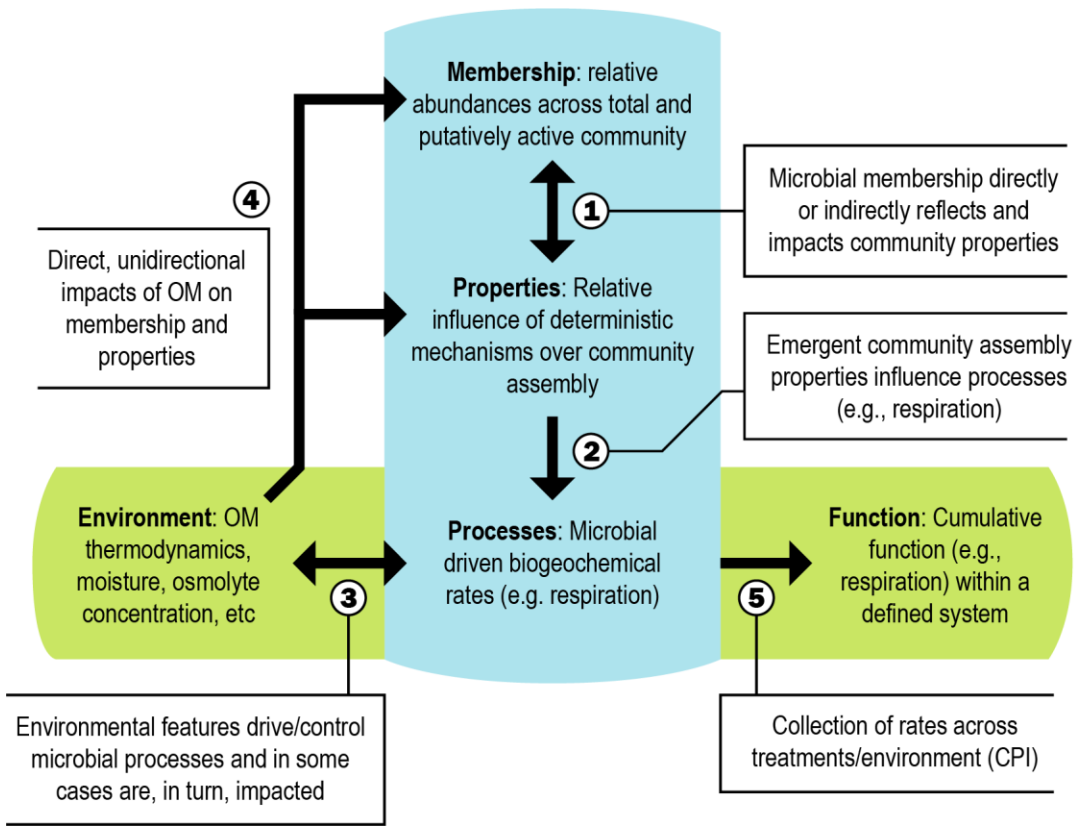
1076

1077 Zhou, J., Liu, W., Deng, Y., Jiang, Y.-H., Xue, K., He, Z., Nostrand, J. D. V., Wu, L., Yang, Y. and
1078 Wang, A.: Stochastic Assembly Leads to Alternative Communities with Distinct Functions in a
1079 Bioreactor Microbial Community, *mBio*, 4(2), <https://doi.org/10.1128/mBio.00584-12>, 2013.

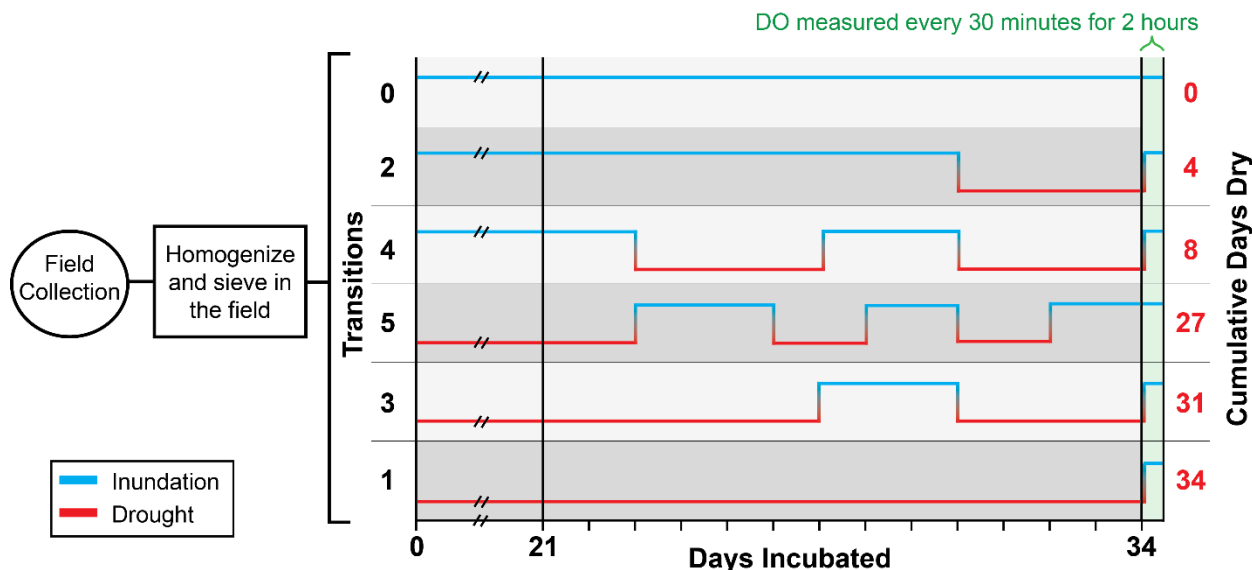
1080

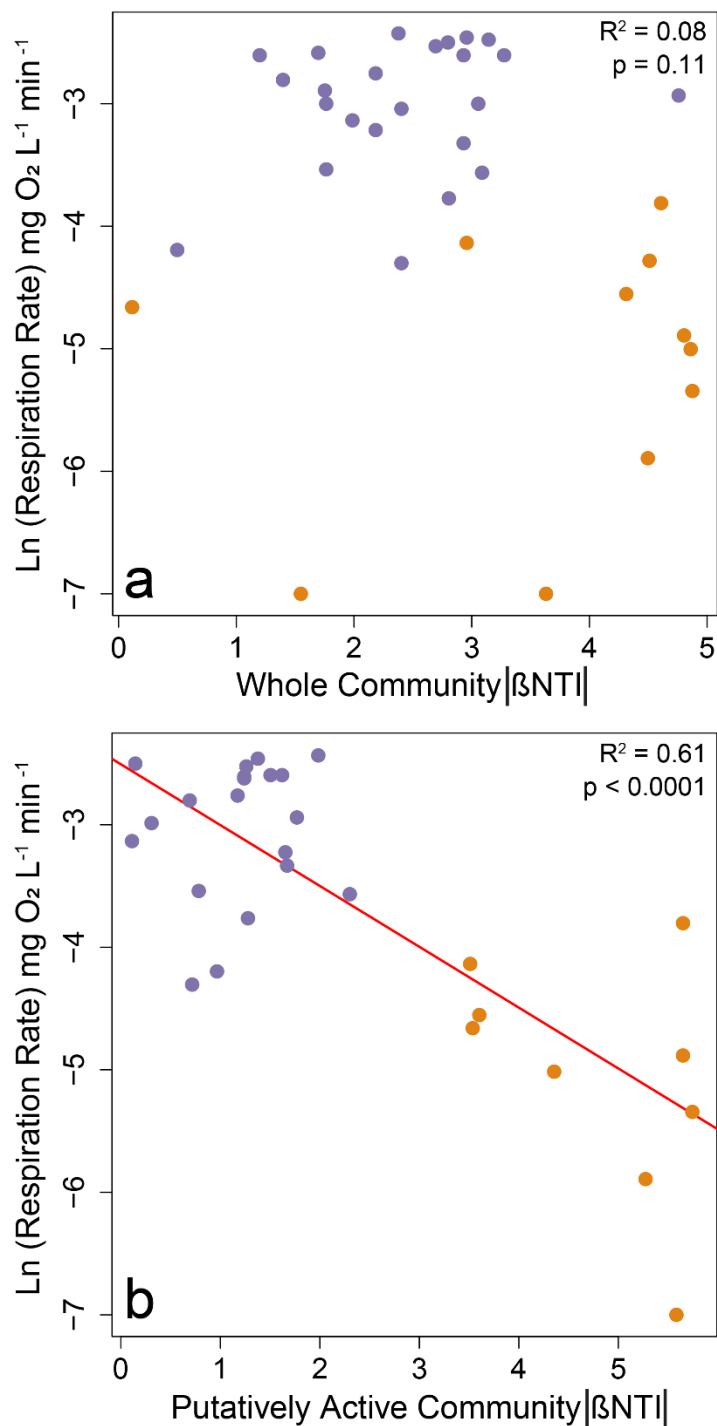
1081

1082 **Figures**
1083



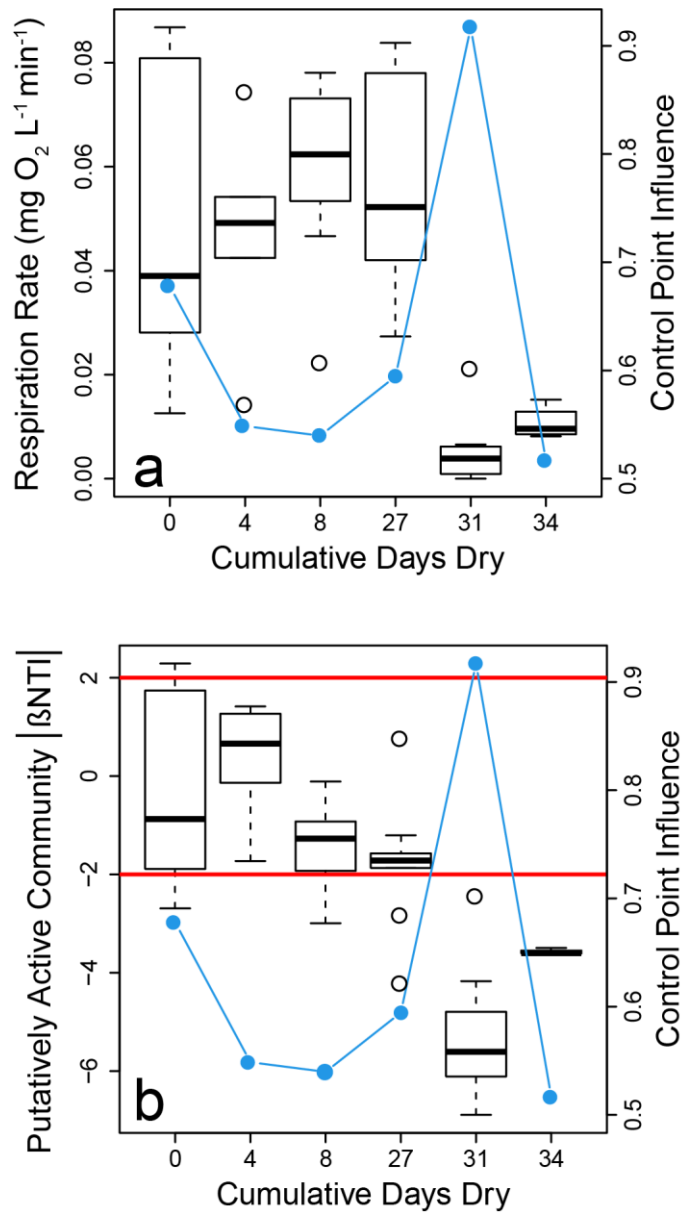
1084
1085
1086 **Figure 1. Integrated conceptual framework.** The conceptual figure (modified from Hall et al. (2018))
1087 details relationships (indicated by numbered arrows) between cumulative properties of the microbial
1088 community (e.g., microbial membership, community assembly properties, biogeochemical rates),
1089 environmental features [e.g., organic matter (OM) thermodynamics], and emergent ecosystem function
1090 [e.g., control point influence (CPI)]. Double headed arrows indicate feedbacks.



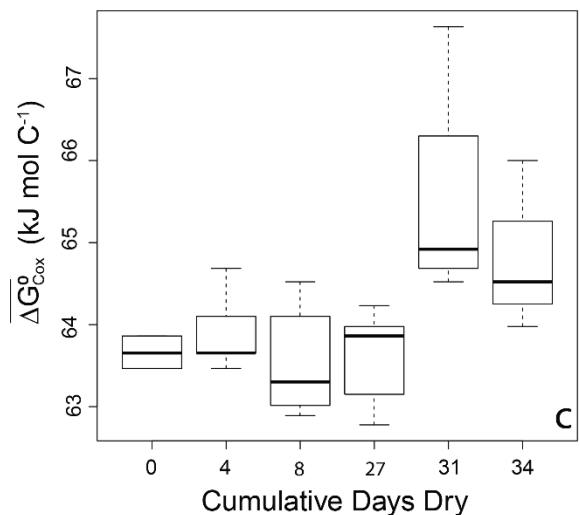
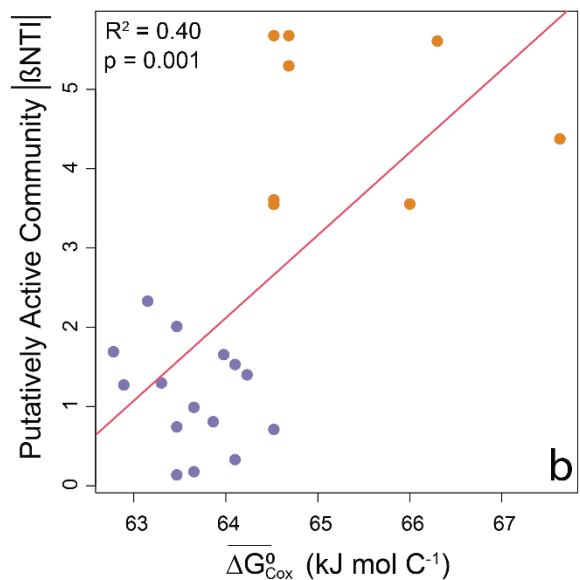
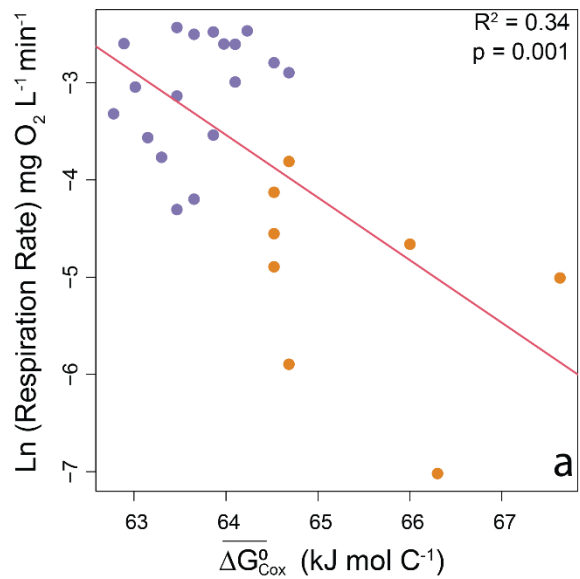


1102
1103
1104
1105
1106
1107
1108
1109
1110
1111

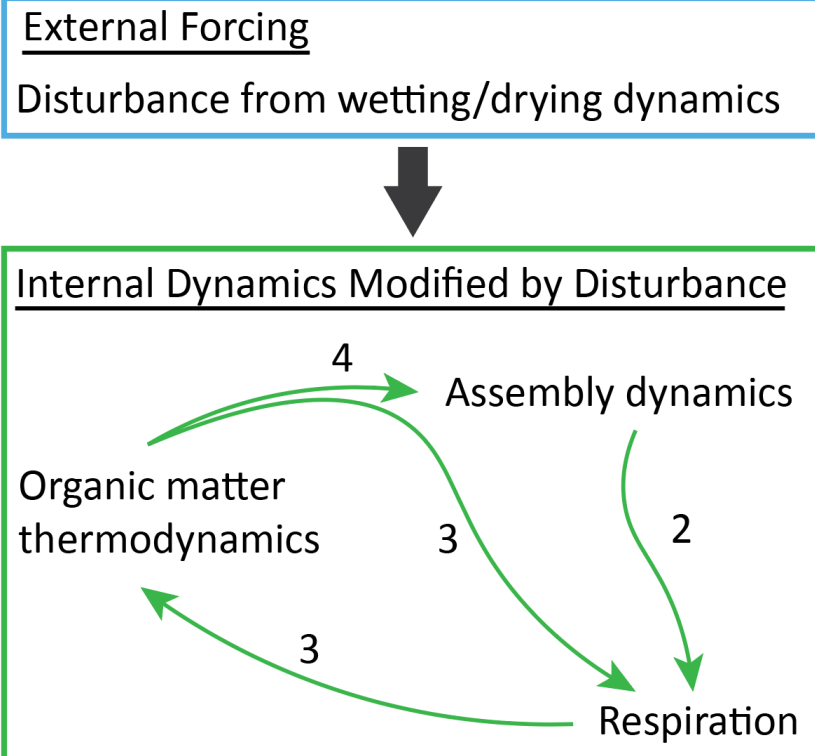
Figure 3. Natural log transformed respiration rates (i.e., O₂ consumption) as a function of the absolute value of β -NTI for (a) whole communities or (b) putatively active communities. Larger absolute values of β -NTI indicate stronger influences of deterministic assembly. Nonlinearity was observed because the respiration rate has a lower limit of 0 such that its relationship with β -NTI was fit as a negative exponential function. The significant regression model is shown as a red line, and statistics are provided on each panel. Treatments with 0, 4, 8, or 27 days dry are shown in purple. Treatments with 31 or 34 days dry are shown in orange.



1112
1113 **Figure 4. Boxplot representations of respiration rate (a) and putatively active community β NTI
1114 (b) distributions as a function of the cumulative number of days reactors were in a dried state.**
1115 Each value along the horizontal axis represents a different experimental treatment. On both panels the
1116 right hand axis provides estimates of control point influence (blue circles and lines) across the
1117 treatments. Horizontal red lines in (b) indicate significance thresholds; values below -2 indicate
1118 deterministic homogenous selection, values above +2 indicate deterministic variable selection, and
1119 values between -2 and +2 indicate stochastic assembly.
1120



1122 **Figure 5. Microbial processes and properties as a function of OM thermodynamics, and impacts**
1123 **of disturbance on OM thermodynamics.** (a) Respiration rates (natural log transformed) decreased
1124 with decreasing favorability for oxidation (larger values of ΔG^0_{Cox}). (b) The strength of deterministic
1125 selection measured as the absolute value of βNTI increased with decreasing favorability for oxidation. Regression
1126 models are shown as red lines and statistics are provided on each panel. (c) Boxplot representations of the
1127 distributions of OM thermodynamics across experimental treatments. Significant increases were observed for
1128 treatments with 31 or 34 cumulative dry days. See text and Figure S7 for a description of statistics. Treatments
1129 with 0, 4, 8, or 27 days dry are shown in purple. Treatments with 31 or 34 days dry are shown in orange.
1130
1131



1132
1133
1134 **Figure 6. Integrated conceptual interpretation of results from this study.** Collectively, our results
1135 indicate that the external forcing imposed by disturbance leads to feedback between assembly of the
1136 putatively active community and respiration rates that is modulated by coupled dynamics in organic
1137 matter thermodynamics. Relative to Fig. 1, here external and internal aspects of the environment are
1138 separated. The arrows within the internal dynamics component are analogous to arrows 2,3, and 4 in
1139 Figure 1. The arrow from external to internal is not considered in Figure 1, and represents the impact of
1140 external forcing on all aspects of the internal system. These impacts are both direct effects of
1141 disturbance and indirect effects mediated through the internal feedback that collectively lead to impacts
1142 of re-wetting that are contingent on desiccation history.